

Search for a new pseudoscalar decaying into a pair of muons in events with a top-quark pair at $\sqrt{s} = 13$ TeV with the ATLAS detector

G. Aad *et al.**
(ATLAS Collaboration)

 (Received 28 April 2023; accepted 18 September 2023; published 28 November 2023)

A search for a new pseudoscalar a -boson produced in events with a top-quark pair, where the a -boson decays into a pair of muons, is performed using $\sqrt{s} = 13$ TeV pp collision data collected with the ATLAS detector at the LHC, corresponding to an integrated luminosity of 139 fb^{-1} . The search targets the final state where only one top quark decays to an electron or muon, resulting in a signature with three leptons $e\mu\mu$ and $\mu\mu\mu$. No significant excess of events above the Standard Model expectation is observed and upper limits are set on two signal models: $pp \rightarrow t\bar{t}a$ and $pp \rightarrow t\bar{t}$ with $t \rightarrow H^\pm b$, $H^\pm \rightarrow W^\pm a$, where $a \rightarrow \mu\mu$, in the mass ranges $15 \text{ GeV} < m_a < 72 \text{ GeV}$ and $120 \text{ GeV} \leq m_{H^\pm} \leq 160 \text{ GeV}$.

DOI: [10.1103/PhysRevD.108.092007](https://doi.org/10.1103/PhysRevD.108.092007)

I. INTRODUCTION

This paper describes a search for the production of a new light pseudoscalar particle decaying into a pair of muons in events with a top-quark pair. Such new particles are well motivated phenomenologically and have been proposed as an explanation for the excess of γ -ray emissions from the center of our galaxy [1–4] in the context of Coy dark matter models [5–7]. They can be colorless solutions of the naturalness problem [8–11]. A light scalar can also render the electroweak phase transition strong first-order, which is one of the ingredients for electroweak baryogenesis [12–14]. These new particles are present in several extensions of the Standard Model (SM), where new light pseudoscalars mix with fields in an extended Higgs sector, which may include additional heavy neutral and charged scalars, inheriting the Yukawa couplings to fermions. In this case, the large coupling to top quarks suggests a search for this new light pseudoscalar produced in events with a top-quark pair [15]. Two scenarios are considered: one where the new light particle a is produced in association with a top-quark pair ($t\bar{t}a, a \rightarrow \mu\mu$) and another where a top quark decays into a new charged Higgs boson that subsequently decays into a new light particle and a W boson ($t \rightarrow H^\pm b$, $H^\pm \rightarrow W^\pm a$, $a \rightarrow \mu\mu$). The search focuses on the mass ranges $15 \text{ GeV} < m_a < 72 \text{ GeV}$

and $120 \text{ GeV} \leq m_{H^\pm} \leq 160 \text{ GeV}$. The high mass resolution achievable for muon pairs provides a distinctive signature to search for and excellent discrimination against most of the background sources. The search targets final states with three leptons, including an electron or muon from a top-quark decay in addition to the two muons from the light pseudoscalar decay. Figure 1 shows representative Feynman diagrams for the signal processes targeted by this search.

This analysis uses data from proton–proton (pp) collisions at a center-of-mass energy of $\sqrt{s} = 13$ TeV collected by the ATLAS experiment during Run 2 (2015 to 2018) of the Large Hadron Collider (LHC), corresponding to an integrated luminosity of 139 fb^{-1} . Previous results include those from a more general search for multilepton signatures by the CMS Collaboration that sets upper limits of 1–10 fb on the production cross section for $t\bar{t}a, a \rightarrow \mu\mu$ at 95% confidence level in the mass ranges $m_a = 15$ –75 GeV and 108–340 GeV [16]. The CMS Collaboration also performed a search for $H^\pm \rightarrow W^\pm a$, $a \rightarrow \mu\mu$ in $t \rightarrow H^\pm b$ decays targeting the mass ranges $m_{H^\pm} = 120$ –160 GeV and $m_a = 15$ –75 GeV, and set upper limits of $(1.9 - 8.6) \times 10^{-6}$ on the branching ratio $\text{B}(t \rightarrow bH^\pm, H^\pm \rightarrow W^\pm a, a \rightarrow \mu\mu)$ at 95% confidence level [17]. Previously, the CDF Collaboration searched for $H^\pm \rightarrow Wa$, $a \rightarrow \tau\tau$ in $t \rightarrow H^\pm b$ decays, targeting the mass ranges $m_{H^\pm} = 90$ –160 GeV and $m_a = 4$ –9 GeV [18].

*Full author list given at the end of the article.

Published by the American Physical Society under the terms of the [Creative Commons Attribution 4.0 International license](https://creativecommons.org/licenses/by/4.0/). Further distribution of this work must maintain attribution to the author(s) and the published article's title, journal citation, and DOI. Funded by SCOAP³.

II. ATLAS DETECTOR

The ATLAS experiment [19] at the LHC is a multipurpose particle detector with a forward–backward symmetric

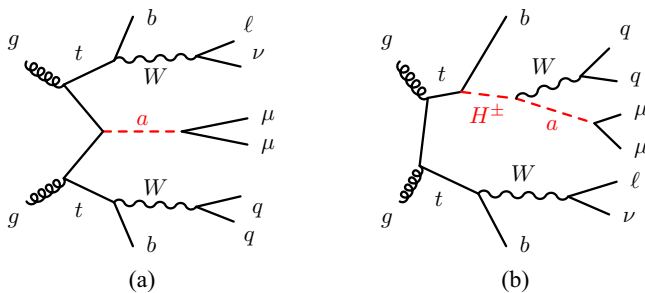


FIG. 1. Feynman diagrams for the leading contributions to the (a) $t\bar{t}a$ process and to the (b) $pp \rightarrow t\bar{t}$ process with $t \rightarrow H^+ b$, $H^+ \rightarrow W^+ a$.

cylindrical geometry and a near 4π coverage in solid angle.¹ It consists of an inner tracking detector (ID) surrounded by a thin superconducting solenoid providing a 2T axial magnetic field, electromagnetic (EM) and hadron calorimeters, and a muon spectrometer. The inner tracking detector covers the pseudorapidity range $|\eta| < 2.5$. It consists of silicon pixel, silicon microstrip, and transition radiation tracking detectors. Lead/liquid-argon (LAr) sampling calorimeters provide EM energy measurements with high granularity. A steel/scintillator-tile hadron calorimeter covers the central pseudorapidity range ($|\eta| < 1.7$). The endcap and forward regions are instrumented with LAr calorimeters for both the EM and hadronic energy measurements up to $|\eta| = 4.9$. The muon spectrometer surrounds the calorimeters and is based on three large superconducting air-core toroidal magnets with eight coils each. The field integral of the toroids ranges between 2.0 and 6.0 Tm across most of the detector. The muon spectrometer includes a system of precision chambers for tracking and fast detectors for triggering. A two-level trigger system is used to select events. The first-level trigger is implemented in hardware and uses a subset of the detector information to accept events at a rate below 100 kHz. This is followed by a software-based trigger that reduces the accepted event rate to 1 kHz on average depending on the data-taking conditions. An extensive software suite [20] is used in data simulation, in the reconstruction and analysis of real and simulated data, in detector operations, and in the trigger and data acquisition systems of the experiment.

III. DATA AND SIMULATED SAMPLES

The analysis uses pp collision data collected with the ATLAS detector in Run 2 of the LHC, at a center-of-mass

¹ATLAS uses a right-handed coordinate system with its origin at the nominal interaction point (IP) in the center of the detector and the z -axis along the beam pipe. The x -axis points from the IP to the center of the LHC ring, and the y -axis points upward. Cylindrical coordinates (r, ϕ) are used in the transverse plane, ϕ being the azimuthal angle around the z -axis. The pseudorapidity is defined in terms of the polar angle θ as $\eta = -\ln \tan(\theta/2)$. Angular distance is measured in units of $\Delta R \equiv \sqrt{(\Delta\eta)^2 + (\Delta\phi)^2}$.

energy of $\sqrt{s} = 13$ TeV, corresponding to a total integrated luminosity of 139 fb^{-1} [21]. Events were recorded using single-lepton triggers with either a low p_T threshold and a lepton isolation requirement, or a higher threshold but a looser identification criterion and without any isolation requirement. The lowest p_T threshold in the single-muon trigger was 20 (26) GeV [22] for data taken in 2015 (2016–2018), while in the single-electron trigger it was 24 (26) GeV [23]. Only events for which the LHC beams were in stable-collision mode and all relevant subsystems were operational are used [24].

Simulated signal and background samples are used to describe background sources, to estimate signal efficiency and acceptance, and to design and optimize the analysis. Monte Carlo (MC) samples were produced using either the full ATLAS detector simulation [25] based on GEANT4 [26] or a faster simulation where the full GEANT4 simulation of the calorimeter response is replaced by a detailed parameterization of the shower shapes [25]. The effects of multiple inelastic interactions in the same and neighboring bunch crossings (pileup) were modeled by overlaying each simulated hard-scattering event with inelastic pp events generated with PYTHIA 8.186 [27] using the NNPDF2.3LO set of parton distribution functions (PDFs) [28] and the A3 set of tuned parameters (tune) [29]. Simulated events are reweighted to match the pileup conditions observed in the full Run 2 dataset. All simulated events are processed through the same reconstruction algorithms and analysis chain as the data. Table I summarizes all the generated samples.

The precision of the matrix element (ME) generators is next-to-leading order (NLO) in quantum chromodynamics (QCD) for most samples. In all samples where the parton shower (PS), hadronization, and multiparton interactions (MPI) were generated with PYTHIA 8, the decays of b - and c -hadrons were simulated using the EvtGen 1.6.0 program [40], and the A14 tune [41] and the NNPDF2.3LO PDF set [28] were used. Several samples were simulated with the Sherpa 2.2 generator [42]. In this setup, NLO-accurate MEs for up to two partons, and MEs with leading-order (LO) accuracy for up to four partons, were calculated with the Comix [43] and OpenLoops libraries. They were matched with the Sherpa parton shower [44] by using the MEPS@NLO prescription [45–48] with the tune developed by the Sherpa authors and based on the NNPDF3.0NNLO set of PDFs [49]. The top-quark mass was set to $m_t = 172.5$ GeV. The $t\bar{t}Z$ sample includes the contribution of $t\bar{t}\gamma^*$ starting at $m_{\ell\ell} > 5$ GeV. The overlap between the $Z(t\bar{t})$ and the $Z\gamma + \text{jets}$ ($t\bar{t}\gamma$) samples is removed following the prescription in Ref. [50].

The $t\bar{t}a$ signal samples were simulated with the MadGraph5_aMC@NLO 2.7.3 generator [51] at NLO precision. The FeynRules [52,53] model used is based on Ref. [54] and it assumes a pseudoscalar coupling between the a -boson and fermions. The simulated signal samples use the

TABLE I. Generator setups for samples used in this analysis. The precision of the ME generator is NLO in QCD if no additional information is provided in parentheses. The higher-order cross section used to normalize these samples is listed in the last column if different from the one in the generator.

Process	ME generator	ME PDF	PS	Normalization
		Signal		
$t\bar{t}a$	MadGraph5_aMC@NLO 2.7.3	NNPDF3.0NLO	PYTHIA 8.210	...
$H^\pm \rightarrow Wa$	MadGraph5_aMC@NLO 2.3.3 (LO)	NNPDF2.3LO	PYTHIA 8.186	...
Backgrounds				
$t\bar{t}Z$	MadGraph5_aMC@NLO [2.3.3]	NNPDF3.0NLO	PYTHIA 8.210	NLO QCD + NLO EW [30]
$t\bar{t}W$	MadGraph5_aMC@NLO 2.3.3	NNPDF3.0NLO	PYTHIA 8.210	NLO QCD + NLO EW [30]
$t\bar{t}H$	POWHEG BOX v2	NNPDF3.0NLO	PYTHIA 8.230	NLO QCD + NLO EW [30]
$WZ + \text{jets}$	Sherpa 2.2.2 (NLO [1j], LO [3j])	NNPDF3.0NNLO	Sherpa 2.2.2	...
tZq	MadGraph5_aMC@NLO 2.3.3	NNPDF3.0NLO	PYTHIA 8.230	...
tWZ	MadGraph5_aMC@NLO 2.3.3	NNPDF3.0NLO	PYTHIA 8.212	...
$ZZ + \text{jets}$	Sherpa 2.2.2 (NLO [1j], LO [3j])	NNPDF3.0NNLO	Sherpa 2.2.2	...
WWZ, WZZ, ZZZ	Sherpa 2.2.2	NNPDF3.0NNLO	Sherpa 2.2.2	...
$t\bar{t}t\bar{t}$	MadGraph5_aMC@NLO 2.3.3	NNPDF3.1NLO	PYTHIA 8.230	NLO QCD + NLO EW [31]
$t\bar{t}$	POWHEG BOX v2	NNPDF3.0NLO	PYTHIA 8.230	NNLO QCD + NNLL [32–38]
$Z + \text{jets}$	Sherpa 2.2.1 (NLO [2j], LO [4j])	NNPDF3.0NNLO	Sherpa 2.2.1	NNLO QCD [39]
$Z\gamma + \text{jets}$	Sherpa 2.2.8 (NLO [1j], LO [3j])	NNPDF3.0NNLO	Sherpa 2.2.8	...
$t\bar{t}\gamma$	MadGraph5_aMC@NLO 2.3.3 (LO)	NNPDF2.3LO	PYTHIA 8.212	...

NNPDF3.0NLO PDF set. Tau-lepton decays of the top-quark pair are explicitly included even though their acceptance is relatively small. The production includes gg -, qg - and $q\bar{q}$ -initiated processes. Diagrams with a single top quark, such as tWa and tqa are not included. The leading-order gg production process is shown in Fig. 1. In the case of $q\bar{q}$ -initiated production, three-body decays $t \rightarrow bWa$ are considered via a Breit–Wigner approximation in the whole mass spectrum of this search. Decays of the top quarks are simulated using the MADSPIN program [55] by setting the parameter BWCUT to at least $(m_t - m_a)/\Gamma_t$, where Γ_t is the top-quark width. The a -boson is simulated with a narrow-width approximation. The events were interfaced to PYTHIA 8.210 [56], which used the A14 tune for modeling of showering and hadronization effects. The simulated mass points correspond to a -boson masses of 12, 16, 20, 25, 30, 40, 50, 60, 70 and 77 GeV.

The $t \rightarrow H^+b$, $H^+ \rightarrow W^+a$ signal samples were simulated using the MadGraph5_aMC@NLO 2.3.3 generator interfaced with PYTHIA 8.186, which used the A14 tune. This leading-order simulation uses the NNPDF2.3LO PDF set. Both H^+ and a were simulated using a narrow-width assumption because the width is always smaller than the detector resolution for the investigated parameter space. The simulated signal samples include the CP -conjugate state of H^+ . The minor contributions from single-top-quark decays are neglected. A two-dimensional grid was chosen for the simulated (H^+, a) masses from 15 GeV to 75 GeV in m_a and from 120 GeV to 160 GeV in m_{H^+} . Mass points were generated in steps of 15 GeV for the a -boson mass and 20 GeV for the H^+ boson mass.

IV. OBJECT AND EVENT SELECTION

Electrons are reconstructed from tracks in the ID associated with topological clusters of energy deposits in the calorimeter [57] and are required to have $p_T > 27$ GeV and $|\eta| < 2.47$. Electrons in the calorimeter barrel–endcap transition region ($1.37 < |\eta| < 1.52$) are excluded. Electrons must satisfy the “medium” likelihood identification criterion and a very tight isolation requirement (“PLVTight”) [57,58], which takes into account calorimeter energy deposits and charged-particle tracks (including the lepton track) in a cone around the lepton direction in order to reject electrons that likely originated from light- or heavy-flavor hadrons. Electron tracks must match the primary vertex of the event,² i.e. they have to satisfy $|z_0 \sin(\theta)| < 0.5$ mm and $|d_0^{\text{sig}}| = |d_0/\sigma(d_0)| < 5$, where z_0 is the longitudinal impact parameter relative to the primary vertex and d_0 [with uncertainty $\sigma(d_0)$] is the transverse impact parameter relative to the beam line.

Muon candidates are identified by matching ID tracks to full tracks or track segments reconstructed in the muon spectrometer, using the “medium” identification criterion [60]. Muons are required to have $p_T > 10$ GeV and $|\eta| < 2.5$. Muon tracks must also satisfy $|z_0 \sin(\theta)| < 0.5$ mm to reject pileup tracks. A “tight” muon selection is defined by additionally requiring that the muon candidate

²The primary vertex is the point at which a pp interaction occurred. If more than one primary vertex is found, the hard-scattering primary vertex is selected as the one with the highest sum of squared transverse momenta of associated tracks [59].

satisfies $|d_0^{\text{sig}}| < 3$ and the isolation criterion ‘‘PFlowLoose’’ with p_T^a -dependent ΔR cone radius [60]. The isolation criterion is corrected for the presence of nearby muons by subtracting from the isolation sum the p_T of a track associated with any other loose muon within the isolation cone of the muon. This correction is particularly important at low m_a , where the angular separation of the two muons from the a -boson decay can be small, less than the cone radius in the isolation calculation. All leptons are required to satisfy $\Delta R(\ell_1, \ell_2) > 0.1$ to reject decay chains of hadrons that produce multiple leptons.

Jets are reconstructed from tracks in the ID and topological energy clusters in the calorimeter [61]. Tracks matched to energy clusters, as well as unmatched energy clusters, are used in a particle-flow algorithm which determines the inputs for an anti- k_t clustering algorithm [62] with a radius parameter of 0.4. Jets are required to satisfy $p_T > 20$ GeV and $|\eta| < 2.5$. The effect of pileup is reduced by an algorithm which uses tracking information to require that the calorimeter-based jets are consistent with originating from the primary vertex [63]. Jets containing b -flavored hadrons (‘‘ b -jets’’) are identified by a multivariate discriminant ‘‘DL1r’’ [64–66] combining track impact parameter values with information from secondary vertices reconstructed within the jet using a deep feed-forward neural network. A working point corresponding to 70% efficiency for identifying b -jets and rejection rates of 9.4 for c -jets and 390 for light-flavor jets measured with simulated $t\bar{t}$ events is used.

An overlap removal procedure is applied to prevent double-counting of objects. The closest jet within $\Delta R_y = \sqrt{(\Delta y)^2 + (\Delta\phi)^2} = 0.2$ of a selected electron is removed, where $y = [(E + p_z)/(E - p_z)]/2$. If the nearest jet surviving that selection is within $\Delta R_y = 0.4$ of an electron, the electron is discarded. Muons are usually removed if they are separated from the nearest jet by $\Delta R_y < 0.4$, since this reduces the background from heavy-flavor decays inside jets. However, if this jet has fewer than three associated tracks, the muon is kept and the jet is removed instead; this avoids an inefficiency for high-energy muons undergoing significant energy loss in the calorimeter. Electrons are removed if they share their track with a muon.

Events are required to have at least one primary vertex with two or more tracks with $p_T > 0.5$ GeV [59] and to have either exactly one electron and two opposite-charge muons, or three muons with total charge ± 1 . Events with electrons are selected with a single-electron trigger and the selected electron must match the object used in the trigger decision. Events with three muons are selected with a single-muon trigger.

Additional selections for muon candidates are used depending on the value of the a -boson mass being considered. The two opposite-charge muons with a reconstructed invariant mass closest to the mass of the hypothesized a -boson are referred to as ‘‘ a -muons.’’ The leading a -muon

is required to satisfy $p_T > 15$ GeV. In events with three muons, the additional muon is interpreted as coming from a top-quark decay and is referred to as the ‘‘top-muon.’’ The top-muon is required to satisfy $p_T > 27$ GeV and match the trigger object used in the decision. Studies with simulated signal samples show that the a -muons are correctly matched to muons from the a -boson decay in more than 98% of the events. All muons in simulation are required to be matched to true muons originating from the prompt decays of vector bosons or a -bosons.

V. ANALYSIS STRATEGY

Events are categorized into mutually exclusive regions defined by the number of muons satisfying the tight identification selection, the number of jets, the number of b -jets and the invariant mass of muon pairs.

The ‘‘signal regions’’ (SR) in both the $e\mu\mu$ and the $\mu\mu\mu$ final states are defined by $12 \text{ GeV} < m_{\mu\mu}^a < 77 \text{ GeV}$, where $m_{\mu\mu}^a$ is the mass of the two a -muons. The range is chosen so as to minimize contamination from processes with $\Upsilon \rightarrow \mu\mu$ decays with the lower bound, and from processes with on-shell $Z \rightarrow \mu\mu$ decays with the upper bound. In order to target events where only one of the top quarks decays to a lepton, the number of jets is required to be at least three and the number of b -jets to be at least one. In the $\mu\mu\mu$ final state, where there are two possible opposite-sign muon pairs, the mass of the ‘‘other’’ pair (not the pair chosen as a -muons), $m_{\mu\mu}^{\text{other}}$, is required to be $m_{\mu\mu}^{\text{other}} < 77 \text{ GeV}$ or $m_{\mu\mu}^{\text{other}} > 107 \text{ GeV}$ in order to reject events with Z bosons. The SR regions are further binned in $m_{\mu\mu}^a$. The width of the bins is chosen to be twice the expected $m_{\mu\mu}^a$ resolution, defined by the Gaussian core’s width in the signal model.

Several ‘‘control regions’’ (CR) are defined in order to target different sources of background. An ‘‘on- Z ’’ control region is defined by requiring either $77 \text{ GeV} < m_{\mu\mu}^a < 107 \text{ GeV}$ or $77 \text{ GeV} < m_{\mu\mu}^{\text{other}} < 107 \text{ GeV}$ but otherwise the same minimum number of jets and b -jets as in the SR. Two on- Z CRs are defined, one in the $e\mu\mu$ final state and another one in the $\mu\mu\mu$ final state. These regions are further divided into events with 3 jets and 1 b -jet, events with 4 jets and 1 b -jet, and events with at least 4 jets and 2 b -jets. The regions with a small number of jets are enriched in WZ events, while the bins with a large number of jets are enriched in $t\bar{t}Z$ events.

Another CR, defined only in the $e\mu\mu$ final state, targets $t\bar{t}$ processes where both top quarks decay leptonically. In this case, one of the two muons is often produced in the nonprompt decay of a heavy-flavor hadron. This muon, called a ‘‘fake muon,’’ is defined as the one with the same electric charge as the electron. Since both top quarks decay leptonically, events in this CR are required to have one or two jets, with exactly one of them being a b -jet. This region is further binned in $p_T^{\mu, \text{fake}}$.

TABLE II. Definition of the analysis regions, split according to the number of leptons, jets, and b -jets, and the invariant mass requirements on muon pairs.

	Signal regions		On-Z control region		$t\bar{t}$ control region
<i>Channel</i>	$e\mu\mu$	$\mu\mu\mu$	$e\mu\mu$	$\mu\mu\mu$	$e\mu\mu$
<i>Binning</i>	$m_{\mu\mu}^a$	$m_{\mu\mu}^a$	$n_{\text{jets}}, n_{b\text{-jets}}$	$n_{\text{jets}}, n_{b\text{-jets}}$	$p_T^{\mu,\text{fake}}$
$n_{\text{electrons}}$	1	0	1	0	1
n_{muons}	2	3	2	3	2
$m_{\mu\mu}$ [GeV]	$12 < m_{\mu\mu}^a < 77$	$12 < m_{\mu\mu}^a < 77$ and $m_{\mu\mu}^{\text{other}} < 77$ or > 107	$77 < m_{\mu\mu}^a < 107$	$77 < m_{\mu\mu}^a < 107$ or $77 < m_{\mu\mu}^{\text{other}} < 107$	$12 < m_{\mu\mu}^a < 77$
n_{jets}			≥ 3		1 or 2
$n_{b\text{-jets}}$			≥ 1		1

In all regions described above, all muons are required to satisfy the tight selection presented in Sec. IV. Events with exactly one of the selected muons failing to satisfy the tight selection criteria are assigned to one of three “isolation sidebands” enriched in events from background processes with nonprompt muons. The three isolation sidebands correspond to different p_T ranges ($10 \text{ GeV} \leq p_T < 20 \text{ GeV}$, $20 \text{ GeV} \leq p_T < 40 \text{ GeV}$, and $p_T \geq 40 \text{ GeV}$) of the muon which does not satisfy the tight selection criteria. The binning of the isolation sidebands is the same as in the corresponding signal and control regions. The regions used in the analysis are summarized in Table II.

VI. BACKGROUND ESTIMATION

Several SM processes can produce final states which satisfy the object and event selections described above. The contributions from these processes are estimated with simulation or data-driven methods.

Background processes with all leptons originating from the prompt decay of vector bosons are described by simulation. The dominant source of background with prompt leptons is $t\bar{t}Z$, the associated production of a Z boson and a $t\bar{t}$ pair where the off-shell Z boson decays into a low-mass muon pair. The normalization of this process is determined by data and largely constrained by the on- Z control region. The same $t\bar{t}Z$ normalization is used for all analysis channels. The categorization of the on- Z CR in number of jets and b -jets allows a precise data-driven determination of the $t\bar{t}Z$ process normalization despite the large contamination from WZ events, which are subleading in the SR, as shown in Fig. 2. Additional subleading sources of background in the SR include single top quarks produced in association with a Z boson (tZq and tWZ), as well as $t\bar{t}W$, $t\bar{t}H$, triboson VVV , and $t\bar{t}t\bar{t}$ processes. The normalization of each background process with prompt leptons other than $t\bar{t}Z$ is determined from simulation.

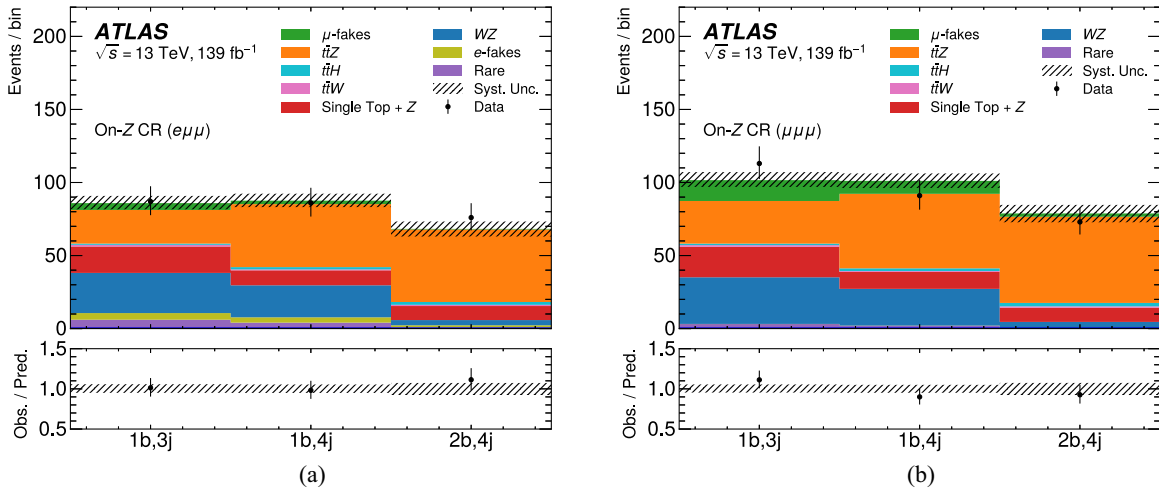


FIG. 2. Comparison between data and expected background for the on- Z control region in the (a) $e\mu\mu$ and (b) $\mu\mu\mu$ final states. The bins correspond to different jet and b -jet multiplicities. Rare background processes include $ZZ + \text{jets}$, WWZ , WZZ , ZZZ , and $t\bar{t}t\bar{t}$. The yields correspond to the values obtained under the background-only hypothesis with the profile likelihood method described in Sec. IX.

Background processes with at least one lepton originating from the nonprompt decay of a hadron, from photon conversion, or from the misidentification of other particles, are described by simulation if the nonprompt lepton is an electron or by a data-driven method if the nonprompt lepton is a muon. Background processes with nonprompt electrons are greatly suppressed by the PLVTight isolation requirement. Nonprompt electrons are further classified depending on whether they originate from photon conversions or from hadrons. Background processes with nonprompt muons provide the largest number of events in the signal regions and the data-driven estimate ensures an accurate description. Simulation studies show that the contribution from processes with more than one nonprompt lepton is negligible.

As described in Sec. V, each channel of the analysis is accompanied by three isolation sidebands enriched in events with nonprompt muons. The three sidebands are distinguished by the p_T of the muon failing the tight selection criteria ($10 \text{ GeV} \leq p_T < 20 \text{ GeV}$, $20 \text{ GeV} \leq p_T < 40 \text{ GeV}$, and $p_T > 40 \text{ GeV}$). The number of events from processes with nonprompt muons in the isolation sidebands is determined by data. The number of events from processes with nonprompt muons in signal and control regions is assumed to be proportional to the number of events in the three sidebands. The proportionality constant, called the fake factor, is different for each of the three sidebands, but otherwise common to all signal and control regions. The fake factors are determined in data and are largely constrained by the $t\bar{t}$ control region, which is divided into the same three bins of $p_T^{\mu, \text{fake}}$. Simulation studies show that background events with nonprompt muons arise mostly ($\approx 90\%$) from $t\bar{t}$ processes where both top quarks decay leptonically. Simulation studies also show

that nearly all other background events with nonprompt muons come from processes with semileptonic decays of heavy-flavor hadrons, akin to $t\bar{t}$ events.

Figure 3 shows the background composition of the two signal regions. Background processes with one nonprompt muon are called μ -fakes and processes with one nonprompt electron are called e -fakes. Rare background processes with prompt leptons are shown together.

VII. SIGNAL MODELING

Simulated samples of the $t\bar{t}a$, $a \rightarrow \mu\mu$ process were generated for 10 different values of the a -boson mass in the range between 12 GeV and 77 GeV. Similarly, in the case of the $t \rightarrow H^+b$, $H^+ \rightarrow W^+a$ signal, samples for up to five different values of the a -boson mass were generated for three different values of m_{H^+} . The number of different mass hypotheses simulated is limited by the computational resources available. The gap between simulated mass hypotheses is, however, much wider than the dimuon mass resolution of the ATLAS detector.

A parameterized model for the $m_{\mu\mu}^a$ spectrum, where $m_{\mu\mu}^a$ is the mass of the two a -muons in each event, is used to probe a -boson mass hypotheses between the values chosen for the simulated samples. The model uses the double Crystal Ball (dCB) probability density function [67]. The parameters of the dCB distribution are evaluated independently for each simulated a -boson mass using a maximum-likelihood fit. Only the Gaussian core's mean and width are observed to vary significantly, while the parameters describing the power-law tails are consistent for all a -boson masses in the range considered in this search. The mean and the width of the Gaussian core vary linearly with the value of the a -boson mass. The signal acceptance

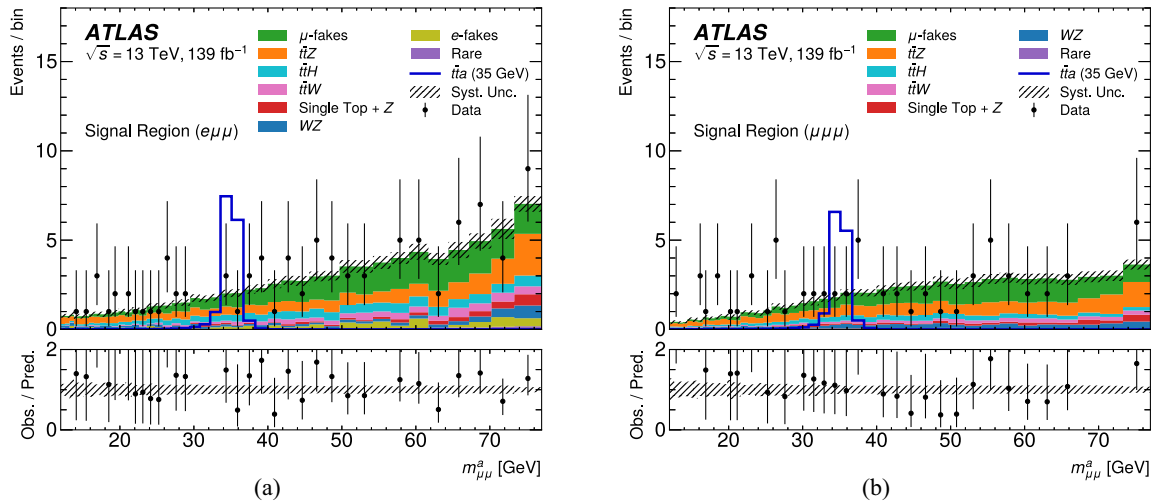


FIG. 3. Dimuon mass distributions for data and expected background in the (a) $e\mu\mu$ and (b) $\mu\mu\mu$ signal regions for the $m_a = 35 \text{ GeV}$ hypothesis. The expected signal distribution is shown assuming $\sigma(t\bar{t}a) \times \text{B}(a \rightarrow \mu\mu) = 4 \text{ fb}^{-1}$. Rare background processes include $ZZ + \text{jets}$, WWZ , WZZ , ZZZ , and $t\bar{t}t\bar{t}$. The yields correspond to the values obtained under the background-only hypothesis with the profile likelihood method described in Section IX.

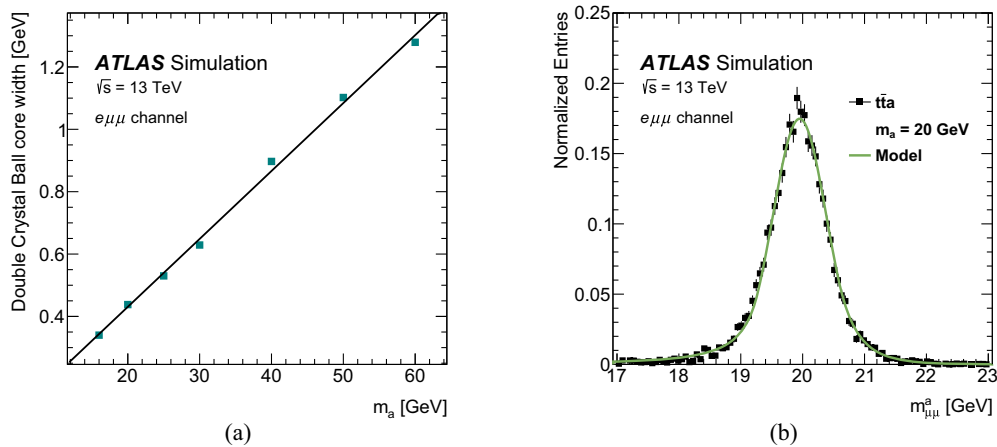


FIG. 4. (a) Fit of the dCB width as a function of the a -boson mass in the $e\mu\mu$ channel. (b) Example fit of the signal using the dCB fit model compared with an independent simulated sample for the $t\bar{t}a$ signal with $m_a = 20$ GeV in the $e\mu\mu$ channel.

times efficiency is also observed to vary linearly with the value of the a -boson mass. The dCB distribution parameters, their linear dependency on the a -boson mass, and the model of the signal acceptance times efficiency are determined separately in the $e\mu\mu$ and $\mu\mu\mu$ channels and for the two signal models $t\bar{t}a$ and $t \rightarrow H^+b$, $H^+ \rightarrow W^+a$ in order to account for the different muon kinematics in the two models. Figure 4 shows the dependency of the dCB width on the value of the a -boson mass in the $e\mu\mu$ channel. It also shows a comparison of the model obtained with the prescription described above and the distribution of events obtained from an independent simulated sample. Similar tests show excellent modeling throughout the whole mass spectrum considered in this search. Once validated, a model built with all the simulated signal mass points was used in the analysis.

VIII. SYSTEMATIC UNCERTAINTIES

Several sources of experimental and modeling systematic uncertainty affecting the signal acceptance and efficiency and the background normalization are considered. The uncertainty in the combined 2015–2018 integrated luminosity is 1.7% [68], obtained using the LUCID-2 detector [69] for the primary luminosity measurements, complemented by measurements using the inner detector and calorimeters. The uncertainty in the number of pileup events is determined by comparing estimates based on the total inelastic cross section measured using either the luminosity detectors or the ID.

Uncertainties in the muon and electron efficiency, momentum scale and resolution are determined from alternative simulations, and from tag-and-probe measurements using $Z \rightarrow \ell\ell$ and $J/\psi \rightarrow \ell\ell$ processes [57,60]. The most important lepton uncertainties in this search are the ones related to the muon identification efficiency. These uncertainties are below 1% in the momentum range considered.

Uncertainties associated with the jet energy scale are evaluated by combining information from test-beam data, LHC collision data and simulation, and the jet energy resolution uncertainty is obtained from measurements of dijet p_T -balance in data and simulation [70]. Additional considerations related to jet flavor, pileup corrections, η dependence and high- p_T jets are included. The efficiency to identify and remove jets from pileup is measured with $Z(\rightarrow\mu^+\mu^-) + \text{jets}$ events in data using techniques similar to those used in Ref. [63]. The uncertainty in tagging b -jets is 2%–10% depending on the jet p_T . The uncertainty in mistagging c -jets (light jets) is 10%–25% (15%–50%) depending on the jet p_T [64–66].

Uncertainties in modeling the background are assessed primarily through variations of the renormalization and factorization scales. The effects of independent variations of the two scales between twice and half their nominal values are considered and their envelope is taken as representative of uncertainties associated with missing higher-order terms in the calculation of the hard-scatter ME. For the leading $t\bar{t}Z$ background process, the scale uncertainties are approximately 5%. Uncertainties associated with the showering and hadronization modeling are assessed through alternative PYTHIA 8 A14 tunes. Uncertainties in the electroweak production of a single top quark in association with a Z boson are estimated by comparing different prescriptions to handle the interference with the $t\bar{t}Z$ process, and are found to have a negligible impact in this search.

Uncertainties associated with the signal processes are found to be largely independent of the a -boson mass hypothesis, and a single uncertainty model is used independently of the signal hypothesis being tested. Uncertainties in modeling the signal acceptance are assessed by varying the renormalization and factorization scales, as described above, as well as through comparison of simulations using either PYTHIA 8 or Herwig 7.1 [71,72] for showering and hadronization. These uncertainties are

approximately 7% for the cross section and 1% for the acceptance. Uncertainties stemming from variations of the proton PDFs are considered for both the signal and background simulations following the NNPDF prescription [28], and are found to have negligible impact on the result.

The systematic uncertainties are much smaller than the data statistical uncertainty. The two largest systematic uncertainties are those related to the muon identification efficiency and the modeling of the $t\bar{t}Z$ background. These uncertainties would have an impact of 2% and 1%, respectively, in the measurement of a hypothetical signal cross section, compared to a statistical uncertainty of approximately 40%–70%, depending on the a -boson mass.

IX. RESULTS

The presence of a signal consistent with the production of $t\bar{t}a$ or $t \rightarrow H^+b, H^+ \rightarrow W^+a$, with $a \rightarrow \mu\mu$ is tested by

comparing the expected background with data in narrow bins of the reconstructed $m_{\mu\mu}^a$. A total of 43 bins between 12 GeV and 77 GeV are used. For simplicity, the same binning is used in both the $e\mu\mu$ and $\mu\mu\mu$ regions. A bin width proportional to the expected width of a detected signal, illustrated in Fig. 4(b), ensures that any signal contribution is highly concentrated in a few bins, while keeping the analysis largely independent of the specific signal mass distribution.

A test statistic is built from a profile likelihood ratio $\tilde{q}_\mu = -2 \ln(\mathcal{L}(\mu, \hat{\theta}_\mu) / \mathcal{L}(\hat{\mu}, \hat{\theta}))$, where the likelihood \mathcal{L} is built starting from the product of Poisson distributions in each analysis channel. The values of the parameters that maximize the likelihood function are $\hat{\mu}$ and $\hat{\theta}$, and the values of the nuisance parameters that maximize the likelihood function for a given value of μ are $\hat{\theta}_\mu$ [73]. The test statistic value is set to zero if the hypothesis μ is lower than the maximum-likelihood estimator $\hat{\mu}$. The expected number of events is parameterized as a function

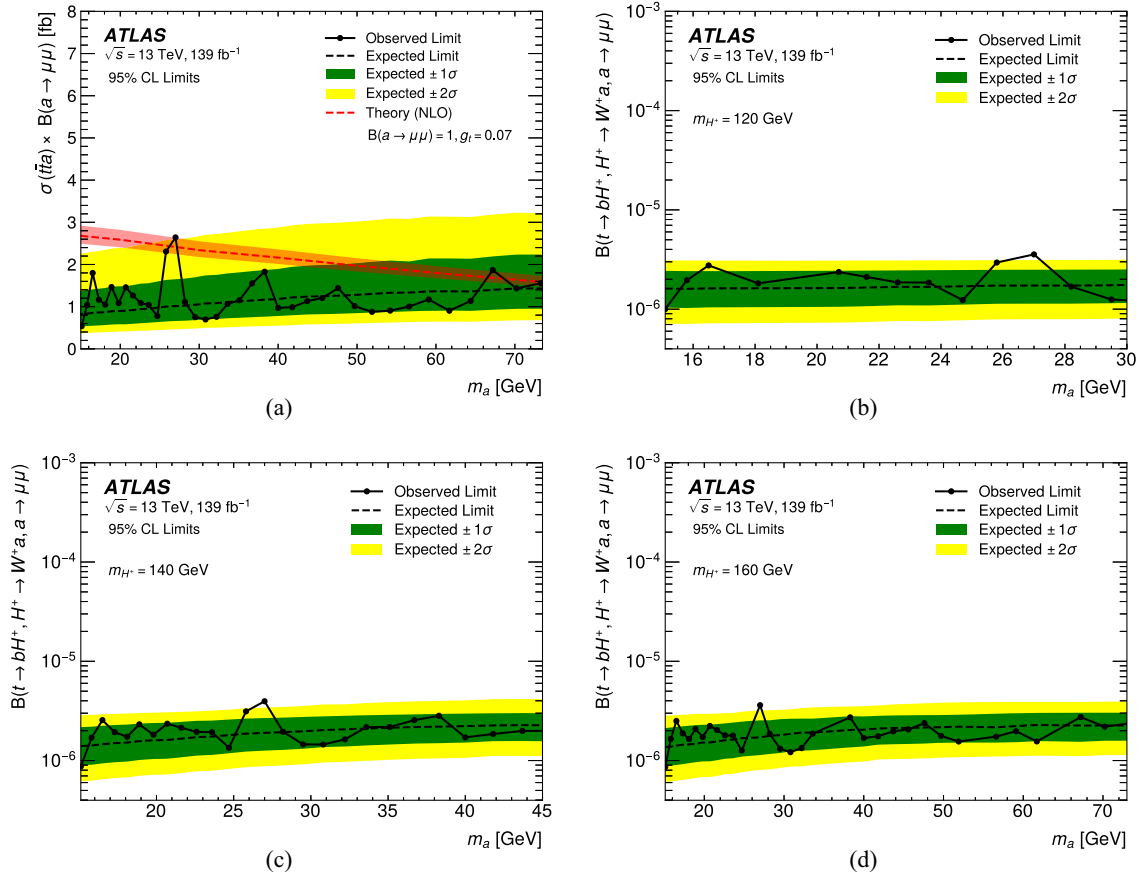


FIG. 5. (a) Expected and observed 95% confidence level (CL) upper limits on the signal cross section shown as a function of m_a for $t\bar{t}a$ production, and a comparison with the cross section predicted by the model described in the text. In (b)–(d), expected and observed 95% CL upper limits on the branching ratio $B(t \rightarrow bH^+, H^+ \rightarrow W^+a, a \rightarrow \mu\mu)$ are shown as a function of m_a for $H^+ \rightarrow W^+a$, assuming a top-pair cross section of $\sigma(pp \rightarrow t\bar{t}) = 833$ pb [32–38], for three values of the charged Higgs boson’s mass: $m_{H^+} = 120$ GeV, $m_{H^+} = 140$ GeV, and $m_{H^+} = 160$ GeV, respectively.

of the signal strength μ , which multiplies a reference signal cross section of 1 fb^{-1} , and a large number of nuisance parameters θ describing the background model and systematic uncertainties. The parameters describing the background model include the ones describing the overall $t\bar{t}Z$ normalization, the background yield from processes with nonprompt leptons in three isolation sidebands independently for each analysis channel, and the three global fake factors. The analysis channels include the 43 bins in each signal region, but also the regions with various numbers of jets and b -jets in the on- Z control region, and the three $p_T^{\mu,\text{fake}}$ regions of the $t\bar{t}$ control region. Hypothesis testing is performed separately for each different value of the a -boson mass. Nuisance parameters describing systematic uncertainties are included by following the prescription in Ref. [74] and have Gaussian constraint terms. Finally, a dedicated set of nuisance parameters is introduced to describe Poisson fluctuations in the background yields estimated from simulation.

As shown in Fig. 3, good agreement is observed between data and the expected background, suggesting the absence of a signal. A hypothetical $t\bar{t}a$ signal with a cross section of 4 fb at $m_a = 35 \text{ GeV}$ is also depicted in Fig. 3, showing the typical concentrated excess that would have been expected from a signal. No significant excess is observed, and the smallest local p -value is 0.008 at $m_a = 27 \text{ GeV}$, corresponding to a local significance of about 2.4σ . The slight excess at $m_a = 27 \text{ GeV}$ is observed in both the $e\mu\mu$ and $\mu\mu\mu$ channels. Upper limits on the signal cross section are determined using the CL_s prescription [73,75] and are shown in Fig. 5(a) together with a comparison with a prediction from a theoretical model for the $t\bar{t}a$ analysis. The model assumes a single coupling $-iy_t g_t a(\bar{t}\gamma_5 t)/\sqrt{2}$, where y_t is the top-quark Yukawa coupling, and the cross section is calculated at NLO precision in QCD. Only $a \rightarrow \mu\mu$ decays are included. A value of $g_t = 0.07$ is chosen as an example in Fig. 5(a) since it approximately reproduces the largest cross section not excluded by this analysis. The uncertainty bands include both the scale and PDF variations. In 2HDM + a models [54], if the heavy Higgs bosons decouple, the coupling g_t is given by $\sin\theta/\tan\beta$, where θ is the mixing angle between the light and heavy pseudoscalar bosons, and $\tan\beta$ is the ratio of the vacuum expectation values of the two scalar doublets.

X. CONCLUSION

A search for a new pseudoscalar a -boson produced in events with a top-quark pair where the a -boson decays into a pair of muons, $a \rightarrow \mu\mu$, is performed. The analysis is based on the dataset of pp collisions at $\sqrt{s} = 13 \text{ TeV}$ recorded by the ATLAS detector in 2015 to 2018, corresponding to an integrated luminosity of 139 fb^{-1} . The search targets the final state where one top quark decays leptonically, resulting in two signal regions with three

leptons, either $e\mu\mu$ or $\mu\mu\mu$, and multiple jets. No significant excess of events above the Standard Model expectation is observed and interpretations in two signal models are considered. Upper limits are set on the cross section for associated production of $t\bar{t}$ and a new pseudoscalar, $pp \rightarrow t\bar{t}a$, times the branching ratio $B(a \rightarrow \mu\mu)$ in the mass range $15 \text{ GeV} < m_a < 72 \text{ GeV}$, and exclude signals with $\sigma(t\bar{t}a)B(a \rightarrow \mu\mu)$ above $0.5\text{--}3 \text{ fb}$ at 95% confidence level. The search also sets upper limits on the branching ratio $B(t \rightarrow bH^+, H^+ \rightarrow W^+ a, a \rightarrow \mu\mu)$ in the range $(0.9\text{--}3.9) \times 10^{-6}$ at 95% confidence level for m_{H^+} between 120 GeV and 160 GeV and m_a between 15 GeV and 72 GeV . The results are largely dominated by statistical uncertainties and are expected to improve as more LHC collision data are collected.

ACKNOWLEDGMENTS

We thank CERN for the very successful operation of the LHC, as well as the support staff from our institutions without whom ATLAS could not be operated efficiently. We acknowledge the support of ANPCyT, Argentina; YerPhI, Armenia; ARC, Australia; BMWFW and FWF, Austria; ANAS, Azerbaijan; CNPq and FAPESP, Brazil; NSERC, NRC and CFI, Canada; CERN; ANID, Chile; CAS, MOST and NSFC, China; Minciencias, Colombia; MEYS CR, Czech Republic; DNRF and DNSRC, Denmark; IN2P3-CNRS and CEA-DRF/IRFU, France; SRNSFG, Georgia; BMBF, HGF and MPG, Germany; GSRI, Greece; RGC and Hong Kong SAR, China; ISF and Benozziyo Center, Israel; INFN, Italy; MEXT and JSPS, Japan; CNRST, Morocco; NWO, Netherlands; RCN, Norway; MEiN, Poland; FCT, Portugal; MNE/IFA, Romania; MESTD, Serbia; MSSR, Slovakia; ARRS and MIZŠ, Slovenia; DSI/NRF, South Africa; MICINN, Spain; SRC and Wallenberg Foundation, Sweden; SERI, SNSF and Cantons of Bern and Geneva, Switzerland; MOST, Taiwan; TENMAK, Türkiye; STFC, United Kingdom; DOE and NSF, United States of America. In addition, individual groups and members have received support from BCKDF, CANARIE, Compute Canada and CRC, Canada; PRIMUS 21/SCI/017 and UNCE SCI/013, Czech Republic; COST, ERC, ERDF, Horizon 2020 and Marie Skłodowska-Curie Actions, European Union; Investissements d'Avenir Labex, Investissements d'Avenir IDEX and ANR, France; DFG and AvH Foundation, Germany; Herakleitos, Thales and Aristeia programmes co-financed by EU-ESF and the Greek NSRF, Greece; BSF-NSF and MINERVA, Israel; Norwegian Financial Mechanism 2014-2021, Norway; NCN and NAWA, Poland; La Caixa Banking Foundation, CERCA Programme Generalitat de Catalunya and PROMETEO and GenT Programmes Generalitat Valenciana, Spain; Göran Gustafssons Stiftelse, Sweden; The Royal Society and Leverhulme Trust, United Kingdom. The crucial computing support from all WLCG partners is acknowledged

gratefully, in particular from CERN, the ATLAS Tier-1 facilities at TRIUMF (Canada), NDGF (Denmark, Norway, Sweden), CC-IN2P3 (France), KIT/GridKA (Germany), INFN-CNAF (Italy), NL-T1 (Netherlands), PIC (Spain),

ASGC (Taiwan), RAL (United Kingdom) and BNL (USA), the Tier-2 facilities worldwide and large non-WLCC resource providers. Major contributors of computing resources are listed in Ref. [76].

-
- [1] L. Goodenough and D. Hooper, Possible evidence for dark matter annihilation in the inner Milky Way from the Fermi gamma ray space telescope, [arXiv:0910.2998](https://arxiv.org/abs/0910.2998).
- [2] D. Hooper and L. Goodenough, Dark matter annihilation in the Galactic center as seen by the Fermi gamma ray space telescope, *Phys. Lett. B* **697**, 412 (2011).
- [3] K. N. Abazajian and M. Kaplinghat, Detection of a gamma-ray source in the Galactic center consistent with extended emission from dark matter annihilation and concentrated astrophysical emission, *Phys. Rev. D* **86**, 083511 (2012).
- [4] T. Daylan, D. P. Finkbeiner, D. Hooper, T. Linden, S. K. N. Portillo, N. L. Rodd, and T. R. Slatyer, The characterization of the gamma-ray signal from the central Milky Way: A case for annihilating dark matter, *Phys. Dark Universe* **12**, 1 (2016).
- [5] C. Boehm, M. J. Dolan, C. McCabe, M. Spannowsky, and C. J. Wallace, Extended gamma-ray emission from coy dark matter, *J. Cosmol. Astropart. Phys.* **05** (2014) 009.
- [6] A. Hektor and L. Marzola, Coy dark matter and the anomalous magnetic moment, *Phys. Rev. D* **90**, 053007 (2014).
- [7] C. Arina, E. DelNobile, and P. Panci, Dark Matter with Pseudoscalar-Mediated Interactions Explains the DAMA Signal and the Galactic Center Excess, *Phys. Rev. Lett.* **114**, 011301 (2015).
- [8] Z. Chacko, H. S. Goh, and R. Harnik, The Twin Higgs: Natural Electroweak Breaking from Mirror Symmetry, *Phys. Rev. Lett.* **96**, 231802 (2006).
- [9] G. Burdman, Z. Chacko, H.-S. Goh, and R. Harnik, Folded supersymmetry and the LEP paradox, *J. High Energy Phys.* **02** (2007) 009.
- [10] G. Burdman, Z. Chacko, R. Harnik, L. deLima, and C. B. Verhaaren, Colorless top partners, a 125 GeV Higgs, and the limits on naturalness, *Phys. Rev. D* **91**, 055007 (2015).
- [11] N. Craig, A. Katz, M. Strassler, and R. Sundrum, Naturalness in the dark at the LHC, *J. High Energy Phys.* **07** (2015) 105.
- [12] S. Profumo, M. J. Ramsey-Musolf, and G. Shaughnessy, Singlet Higgs phenomenology and the electroweak phase transition, *J. High Energy Phys.* **08** (2007) 010.
- [13] K. Ghorbani and P. H. Ghorbani, Strongly first-order phase transition in real singlet scalar dark matter model, *J. Phys. G* **47**, 015201 (2020).
- [14] T. Robens and T. Stefaniak, Status of the Higgs singlet extension of the standard model after LHC run 1, *Eur. Phys. J. C* **75**, 104 (2015).
- [15] M. Casolino, T. Farooque, A. Juste, T. Liu, and M. Spannowsky, Probing a light CP -odd scalar in di-top-associated production at the LHC, *Eur. Phys. J. C* **75**, 498 (2015).
- [16] CMS Collaboration, Search for physics beyond the standard model in multilepton final states in proton-proton collisions at $\sqrt{s} = 13$ TeV, *J. High Energy Phys.* **03** (2020) 051.
- [17] CMS Collaboration, Search for a Light Charged Higgs Boson Decaying to a W Boson and a CP -Odd Higgs Boson in Final States with $e\mu\mu$ or $\mu\mu\mu$ in Proton-Proton Collisions at $\sqrt{s} = 13$ TeV, *Phys. Rev. Lett.* **123**, 131802 (2019).
- [18] CDF Collaboration, Search for a Very Light CP -odd Higgs Boson in Top Quark Decays from $p\bar{p}$ Collisions at 1.96 TeV, *Phys. Rev. Lett.* **107**, 031801 (2011).
- [19] ATLAS Collaboration, The ATLAS experiment at the CERN Large Hadron Collider, *J. Instrum.* **3**, S08003 (2008).
- [20] ATLAS Collaboration, The ATLAS Collaboration software and firmware, Report No. ATL-SOFT-PUB-2021-001, 2021, <https://cds.cern.ch/record/2767187>.
- [21] ATLAS Collaboration, Luminosity determination in pp collisions at $\sqrt{s} = 13$ TeV using the ATLAS detector at the LHC, [arXiv:2212.09379](https://arxiv.org/abs/2212.09379).
- [22] ATLAS Collaboration, Performance of the ATLAS muon triggers in Run 2, *J. Instrum.* **15**, P09015 (2020).
- [23] ATLAS Collaboration, Performance of electron and photon triggers in ATLAS during LHC Run 2, *Eur. Phys. J. C* **80**, 47 (2020).
- [24] ATLAS Collaboration, ATLAS data quality operations and performance for 2015–2018 data-taking, *J. Instrum.* **15**, P04003 (2020).
- [25] ATLAS Collaboration, The ATLAS simulation infrastructure, *Eur. Phys. J. C* **70**, 823 (2010).
- [26] GEANT4 Collaboration, GEANT4—A simulation toolkit, *Nucl. Instrum. Methods Phys. Res., Sect. A* **506**, 250 (2003).
- [27] T. Sjöstrand, S. Mrenna, and P. Skands, A brief introduction to PYTHIA 8.1, *Comput. Phys. Commun.* **178**, 852 (2008).
- [28] R. D. Ball *et al.*, Parton distributions with LHC data, *Nucl. Phys.* **B867**, 244 (2013).
- [29] ATLAS Collaboration, The PYTHIA 8 A3 tune description of ATLAS minimum bias and inelastic measurements incorporating the Donnachie–Landshoff diffractive model, Report No. ATL-PHYS-PUB-2016-017, 2016, <https://cds.cern.ch/record/2206965>.
- [30] D. de Florian *et al.*, Handbook of LHC Higgs cross sections: 4. Deciphering the nature of the Higgs sector, [arXiv:1610.07922](https://arxiv.org/abs/1610.07922).
- [31] R. Frederix, D. Pagani, and M. Zaro, Large NLO corrections in $t\bar{t}W^\pm$ and $t\bar{t}t\bar{t}$ hadroproduction from supposedly sub-leading EW contributions, *J. High Energy Phys.* **02** (2018) 031.

- [32] M. Beneke, P. Falgari, S. Klein, and C. Schwinn, Hadronic top-quark pair production with NNLL threshold resummation, *Nucl. Phys.* **B855**, 695 (2012).
- [33] M. Cacciari, M. Czakon, M. Mangano, A. Mitov, and P. Nason, Top-pair production at hadron colliders with next-to-next-to-leading logarithmic soft-gluon resummation, *Phys. Lett. B* **710**, 612 (2012).
- [34] P. Barnreuther, M. Czakon, and A. Mitov, Percent-Level-Precision Physics at the Tevatron: Next-to-Next-to-Leading Order QCD Corrections to $q\bar{q} \rightarrow t\bar{t} + X$, *Phys. Rev. Lett.* **109**, 132001 (2012).
- [35] M. Czakon and A. Mitov, NNLO corrections to top-pair production at hadron colliders: The all-fermionic scattering channels, *J. High Energy Phys.* **12** (2012) 054.
- [36] M. Czakon and A. Mitov, NNLO corrections to top pair production at hadron colliders: The quark-gluon reaction, *J. High Energy Phys.* **01** (2013) 080.
- [37] M. Czakon, P. Fiedler, and A. Mitov, Total Top-Quark Pair-Production Cross Section at Hadron Colliders Through $\mathcal{O}(\alpha_s^4)$, *Phys. Rev. Lett.* **110**, 252004 (2013).
- [38] M. Czakon and A. Mitov, `Top++`: A program for the calculation of the top-pair cross-section at hadron colliders, *Comput. Phys. Commun.* **185**, 2930 (2014).
- [39] C. Anastasiou, L. J. Dixon, K. Melnikov, and F. Petriello, High-precision QCD at hadron colliders: Electroweak gauge boson rapidity distributions at next-to-next-to leading order, *Phys. Rev. D* **69**, 094008 (2004).
- [40] D. J. Lange, The `EvtGen` particle decay simulation package, *Nucl. Instrum. Methods Phys. Res., Sect. A* **462**, 152 (2001).
- [41] ATLAS Collaboration, ATLAS `PYTHIA 8` tunes to 7 TeV data, Report No. ATL-PHYS-PUB-2014-021, 2014, <https://cds.cern.ch/record/1966419>.
- [42] E. Bothmann *et al.*, Event generation with `Sherpa 2.2`, *SciPost Phys.* **7**, 034 (2019).
- [43] T. Gleisberg and S. Höche, `Comix`, A new matrix element generator, *J. High Energy Phys.* **12** (2008) 039.
- [44] S. Schumann and F. Krauss, A parton shower algorithm based on Catani-Seymour dipole factorisation, *J. High Energy Phys.* **03** (2008) 038.
- [45] S. Höche, F. Krauss, M. Schönherr, and F. Siegert, A critical appraisal of NLO + PS matching methods, *J. High Energy Phys.* **09** (2012) 049.
- [46] S. Höche, F. Krauss, M. Schönherr, and F. Siegert, QCD matrix elements + parton showers. The NLO case, *J. High Energy Phys.* **04** (2013) 027.
- [47] S. Catani, F. Krauss, B. R. Webber, and R. Kuhn, QCD matrix elements + parton showers, *J. High Energy Phys.* **11** (2001) 063.
- [48] S. Höche, F. Krauss, S. Schumann, and F. Siegert, QCD matrix elements and truncated showers, *J. High Energy Phys.* **05** (2009) 053.
- [49] R. D. Ball *et al.* (NNPDF Collaboration), Parton distributions for the LHC Run II, *J. High Energy Phys.* **04** (2015) 040.
- [50] J. Krause and F. Siegert, NLO QCD predictions for $Z + \gamma +$ jets production with `Sherpa`, *Eur. Phys. J. C* **78**, 161 (2018).
- [51] J. Alwall, R. Frederix, S. Frixione, V. Hirschi, F. Maltoni, O. Mattelaer, H.-S. Shao, T. Stelzer, P. Torrielli, and M. Zaro, The automated computation of tree-level and next-to-leading order differential cross sections, and their matching to parton shower simulations, *J. High Energy Phys.* **07** (2014) 079.
- [52] N. D. Christensen and C. Duhr, `FeynRules`—Feynman rules made easy, *Comput. Phys. Commun.* **180**, 1614 (2009).
- [53] A. Alloul, N. D. Christensen, C. Degrande, C. Duhr, and B. Fuks, `FeynRules 2.0`—A complete toolbox for tree-level phenomenology, *Comput. Phys. Commun.* **185**, 2250 (2014).
- [54] M. Bauer, U. Haisch, and F. Kahlhoefer, Simplified dark matter models with two Higgs doublets: I. Pseudoscalar mediators, *J. High Energy Phys.* **05** (2017) 138.
- [55] P. Artoisenet, R. Frederix, O. Mattelaer, and R. Rietkerk, Automatic spin-entangled decays of heavy resonances in Monte Carlo simulations, *J. High Energy Phys.* **03** (2013) 015.
- [56] T. Sjöstrand, S. Ask, J. R. Christiansen, R. Corke, N. Desai, P. Ilten, S. Mrenna, S. Prestel, C. O. Rasmussen, and P. Z. Skands, An introduction to `PYTHIA 8.2`, *Comput. Phys. Commun.* **191**, 159 (2015).
- [57] ATLAS Collaboration, Electron and photon performance measurements with the ATLAS detector using the 2015–2017 LHC proton–proton collision data, *J. Instrum.* **14**, P12006 (2019).
- [58] ATLAS Collaboration, Evidence for the associated production of the Higgs boson and a top quark pair with the ATLAS detector, *Phys. Rev. D* **97**, 072003 (2018).
- [59] ATLAS Collaboration, Reconstruction of primary vertices at the ATLAS experiment in Run 1 proton–proton collisions at the LHC, *Eur. Phys. J. C* **77**, 332 (2017).
- [60] ATLAS Collaboration, Muon reconstruction and identification efficiency in ATLAS using the full Run 2 pp collision data set at $\sqrt{s} = 13$ TeV, *Eur. Phys. J. C* **81**, 578 (2021).
- [61] ATLAS Collaboration, Topological cell clustering in the ATLAS calorimeters and its performance in LHC Run 1, *Eur. Phys. J. C* **77**, 490 (2017).
- [62] M. Cacciari, G. P. Salam, and G. Soyez, The anti- k_r jet clustering algorithm, *J. High Energy Phys.* **04** (2008) 063.
- [63] ATLAS Collaboration, Performance of pile-up mitigation techniques for jets in pp collisions at $\sqrt{s} = 8$ TeV using the ATLAS detector, *Eur. Phys. J. C* **76**, 581 (2016).
- [64] ATLAS Collaboration, ATLAS b -jet identification performance and efficiency measurement with $t\bar{t}$ events in pp collisions at $\sqrt{s} = 13$ TeV, *Eur. Phys. J. C* **79**, 970 (2019).
- [65] ATLAS Collaboration, Measurement of b -tagging efficiency of c -jets in $t\bar{t}$ events using a likelihood approach with the ATLAS detector, Report No. ATLAS-CONF-2018-001, 2018, <https://cds.cern.ch/record/2306649>.
- [66] ATLAS Collaboration, Calibration of light-flavour b -jet mistagging rates using ATLAS proton–proton collision data at $\sqrt{s} = 13$ TeV, Report No. ATLAS-CONF-2018-006, 2018, <https://cds.cern.ch/record/2314418>.
- [67] M. Oreglia, A study of the reactions $\psi' \rightarrow \gamma\gamma\psi$, Ph.D. thesis, Stanford University, 1980 [Report No. SLAC-236].
- [68] ATLAS Collaboration, Luminosity monitoring using $Z \rightarrow \ell^+\ell^-$ events at $\sqrt{s} = 13$ TeV with the ATLAS detector, Report No. ATL-DAPR-PUB-2021-001, 2021, <https://cds.cern.ch/record/2752951>.
- [69] G. Avoni *et al.*, The new LUCID-2 detector for luminosity measurement and monitoring in ATLAS, *J. Instrum.* **13**, P07017 (2018).

- [70] ATLAS Collaboration, Jet energy scale and resolution measured in proton–proton collisions at $\sqrt{s} = 13$ TeV with the ATLAS detector, *Eur. Phys. J. C* **81**, 689 (2020).
- [71] M. Bahr *et al.*, Herwig++ physics and manual, *Eur. Phys. J. C* **58**, 639 (2008).
- [72] J. Bellm *et al.*, Herwig 7.0/Herwig++ 3.0 release note, *Eur. Phys. J. C* **76**, 196 (2016).
- [73] G. Cowan, K. Cranmer, E. Gross, and O. Vitells, Asymptotic formulae for likelihood-based tests of new physics, *Eur. Phys. J. C* **71**, 1554 (2011).
- [74] K. Cranmer, Practical statistics for the LHC, in *Proceedings of the 2011 European School of High-Energy Physics* (2014), p. 267, [arXiv:1503.07622](https://arxiv.org/abs/1503.07622).
- [75] A. L. Read, Presentation of search results: The CL(s) technique, *J. Phys. G* **28**, 2693 (2002).
- [76] ATLAS Collaboration, ATLAS Computing acknowledgements, Report No. ATL-SOFT-PUB-2021-003, 2021, <https://cds.cern.ch/record/2776662>.

G. Aad¹⁰², B. Abbott¹²⁰, K. Abeling⁵⁵, N. J. Abicht⁴⁹, S. H. Abidi²⁹, A. Aboulhorma^{35e}, H. Abramowicz¹⁵¹, H. Abreu¹⁵⁰, Y. Abulaiti¹¹⁷, A. C. Abusleme Hoffmann^{137a}, B. S. Acharya^{69a,69b}, C. Adam Bourdarios⁴, L. Adamczyk^{86a}, L. Adamek¹⁵⁵, S. V. Addepalli²⁶, M. J. Addison¹⁰¹, J. Adelman¹¹⁵, A. Adiguzel^{21c}, T. Adye¹³⁴, A. A. Affolder¹³⁶, Y. Afik³⁶, M. N. Agaras¹³, J. Agarwala^{73a,73b}, A. Aggarwal¹⁰⁰, C. Agheorghiesei^{27c}, A. Ahmad³⁶, F. Ahmadov^{38,c}, W. S. Ahmed¹⁰⁴, S. Ahuja⁹⁵, X. Ai^{62a}, G. Aielli^{76a,76b}, A. Aikot¹⁶³, M. Ait Tamlihat^{35e}, B. Aitbenkikh^{35a}, I. Aizenberg¹⁶⁹, M. Akbiyik¹⁰⁰, T. P. A. Åkesson⁹⁸, A. V. Akimov³⁷, D. Akiyama¹⁶⁸, N. N. Akolkar²⁴, K. Al Khoury⁴¹, G. L. Alberghi^{23b}, J. Albert¹⁶⁵, P. Albicocco⁵³, G. L. Albouy⁶⁰, S. Alderweireldt⁵², M. Aleksa³⁶, I. N. Aleksandrov³⁸, C. Alexa^{27b}, T. Alexopoulos¹⁰, A. Alfonsi¹¹⁴, F. Alfonsi^{23b}, M. Algren⁵⁶, M. Alhroob¹²⁰, B. Ali¹³², H. M. J. Ali⁹¹, S. Ali¹⁴⁸, S. W. Alibocus⁹², M. Aliev¹⁴⁵, G. Alimonti^{71a}, W. Alkakhi⁵⁵, C. Allaire⁶⁶, B. M. M. Allbrooke¹⁴⁶, J. F. Allen⁵², C. A. Allendes Flores^{137f}, P. P. Allport²⁰, A. Aloisio^{72a,72b}, F. Alonso⁹⁰, C. Alpigiani¹³⁸, M. Alvarez Estevez⁹⁹, A. Alvarez Fernandez¹⁰⁰, M. Alves Cardoso⁵⁶, M. G. Alviggi^{72a,72b}, M. Aly¹⁰¹, Y. Amaral Coutinho^{83b}, A. Ambler¹⁰⁴, C. Amelung³⁶, M. Amerl¹⁰¹, C. G. Ames¹⁰⁹, D. Amidei¹⁰⁶, S. P. Amor Dos Santos^{130a}, K. R. Amos¹⁶³, V. Ananiev¹²⁵, C. Anastopoulos¹³⁹, T. Andeen¹¹, J. K. Anders³⁶, S. Y. Andrean^{47a,47b}, A. Andreatza^{71a,71b}, S. Angelidakis⁹, A. Angerami^{41,d}, A. V. Anisenkov³⁷, A. Annovi^{74a}, C. Antel⁵⁶, M. T. Anthony¹³⁹, E. Antipov¹⁴⁵, M. Antonelli⁵³, D. J. A. Antrim^{17a}, F. Anulli^{75a}, M. Aoki⁸⁴, T. Aoki¹⁵³, J. A. Aparisi Pozo¹⁶³, M. A. Aparo¹⁴⁶, L. Aperio Bella⁴⁸, C. Appelt¹⁸, A. Apyan²⁶, N. Aranzabal³⁶, C. Arcangeletti⁵³, A. T. H. Arce⁵¹, E. Arena⁹², J.-F. Arguin¹⁰⁸, S. Argyropoulos⁵⁴, J.-H. Arling⁴⁸, O. Arnaez⁴, H. Arnold¹¹⁴, Z. P. Arrubarrena Tame¹⁰⁹, G. Artoni^{75a,75b}, H. Asada¹¹¹, K. Asai¹¹⁸, S. Asai¹⁵³, N. A. Asbah⁶¹, J. Assahsah^{35d}, K. Assamagan²⁹, R. Astalos^{28a}, S. Atashi¹⁶⁰, R. J. Atkin^{33a}, M. Atkinson¹⁶², N. B. Atlay¹⁸, H. Atmani^{62b}, P. A. Atmasiddha¹⁰⁶, K. Augsten¹³², S. Auricchio^{72a,72b}, A. D. Auriol²⁰, V. A. Austrup¹⁰¹, G. Avolio³⁶, K. Axiotis⁵⁶, G. Azuelos^{108,e}, D. Babal^{28b}, H. Bachacou¹³⁵, K. Bachas^{152,f}, A. Bachiu³⁴, F. Backman^{47a,47b}, A. Badae⁶¹, P. Bagnaia^{75a,75b}, M. Bahmani¹⁸, A. J. Bailey¹⁶³, V. R. Bailey¹⁶², J. T. Baines¹³⁴, L. Baines⁹⁴, C. Bakalis¹⁰, O. K. Baker¹⁷², E. Bakos¹⁵, D. Bakshi Gupta⁸, V. Balakrishnan¹²⁰, R. Balasubramanian¹¹⁴, E. M. Baldin³⁷, P. Balek^{86a}, E. Ballabene^{23b,23a}, F. Balli¹³⁵, L. M. Baltes^{63a}, W. K. Balunas³², J. Balz¹⁰⁰, E. Banas⁸⁷, M. Bandieramonte¹²⁹, A. Bandyopadhyay²⁴, S. Bansal²⁴, L. Barak¹⁵¹, M. Barakat⁴⁸, E. L. Barberio¹⁰⁵, D. Barberis^{57b,57a}, M. Barbero¹⁰², G. Barbour⁹⁶, K. N. Barends^{33a}, T. Barillari¹¹⁰, M.-S. Barisits³⁶, T. Barklow¹⁴³, P. Baron¹²², D. A. Baron Moreno¹⁰¹, A. Baroncelli^{62a}, G. Barone²⁹, A. J. Barr¹²⁶, J. D. Barr⁹⁶, L. Barranco Navarro^{47a,47b}, F. Barreiro⁹⁹, J. Barreiro Guimarães da Costa^{14a}, U. Barron¹⁵¹, M. G. Barros Teixeira^{130a}, S. Barsov³⁷, F. Bartels^{63a}, R. Bartoldus¹⁴³, A. E. Barton⁹¹, P. Bartos^{28a}, A. Basan¹⁰⁰, M. Baselga⁴⁹, A. Bassalat^{66,g}, M. J. Basso^{156a}, C. R. Basson¹⁰¹, R. L. Bates⁵⁹, S. Batlamous^{35e}, J. R. Batley³², B. Batool¹⁴¹, M. Battaglia¹³⁶, D. Battulga¹⁸, M. Bauge^{75a,75b}, M. Bauer³⁶, P. Bauer²⁴, L. T. Bazzano Hurrell³⁰, J. B. Beacham⁵¹, T. Beau¹²⁷, P. H. Beauchemin¹⁵⁸, F. Becherer⁵⁴, P. Bechtel²⁴, H. P. Beck^{19,h}, K. Becker¹⁶⁷, A. J. Beddall⁸², V. A. Bednyakov³⁸, C. P. Bee¹⁴⁵, L. J. Beemster¹⁵, T. A. Beermann³⁶, M. Begalli^{83d}, M. Begel²⁹, A. Behera¹⁴⁵, J. K. Behr⁴⁸, J. F. Beirer⁵⁵, F. Beisiegel²⁴, M. Belfkir¹⁵⁹, G. Bella¹⁵¹, L. Bellagamba^{23b}, A. Bellerive³⁴, P. Bellos²⁰, K. Beloborodov³⁷, N. L. Belyaev³⁷, D. Benchekroun^{35a}, F. Bendebba^{35a}, Y. Benhammou¹⁵¹, M. Benoit²⁹, J. R. Bensinger²⁶, S. Bentvelsen¹¹⁴, L. Beresford⁴⁸, M. Beretta⁵³, E. Bergeas Kuutmann¹⁶¹, N. Berger⁴, B. Bergmann¹³², J. Beringer^{17a}, G. Bernardi⁵, C. Bernius¹⁴³

F. U. Bernlochner²⁴ F. Bernon^{36,102} T. Berry⁹⁵ P. Berta¹³³ A. Berthold⁵⁰ I. A. Bertram⁹¹ S. Bethke¹¹⁰
A. Betti^{75a,75b} A. J. Bevan⁹⁴ M. Bhamjee^{33c} S. Bhatta¹⁴⁵ D. S. Bhattacharya¹⁶⁶ P. Bhattacharai¹⁴³
V. S. Bhopatkar¹²¹ R. Bi^{29,i} R. M. Bianchi¹²⁹ G. Bianco^{23b,23a} O. Biebel¹⁰⁹ R. Bielski¹²³ M. Biglietti^{77a}
T. R. V. Billoud¹³² M. Bindi⁵⁵ A. Bingul^{21b} C. Bini^{75a,75b} A. Biondini⁹² C. J. Birch-sykes¹⁰¹ G. A. Bird^{20,134}
M. Birman¹⁶⁹ M. Biros¹³³ T. Bisanz⁴⁹ E. Bisceglie^{43b,43a} D. Biswas¹⁴¹ A. Bitadze¹⁰¹ K. Bjørke¹²⁵
I. Bloch⁴⁸ C. Blocker²⁶ A. Blue⁵⁹ U. Blumenschein⁹⁴ J. Blumenthal¹⁰⁰ G. J. Bobbink¹¹⁴
V. S. Bobrovnikov³⁷ M. Boehler⁵⁴ B. Boehm¹⁶⁶ D. Bogavac³⁶ A. G. Bogdanchikov³⁷ C. Bohm^{47a}
V. Boisvert⁹⁵ P. Bokan⁴⁸ T. Bold^{86a} M. Bomben⁵ M. Bona⁹⁴ M. Boonekamp¹³⁵ C. D. Booth⁹⁵
A. G. Borbély⁵⁹ I. S. Bordulev³⁷ H. M. Borecka-Bielska¹⁰⁸ L. S. Borgna⁹⁶ G. Borissov⁹¹ D. Bortoletto¹²⁶
D. Boscherini^{23b} M. Bosman¹³ J. D. Bossio Sola³⁶ K. Bouaouda^{35a} N. Bouchhar¹⁶³ J. Boudreau¹²⁹
E. V. Bouhova-Thacker⁹¹ D. Boumediene⁴⁰ R. Bouquet⁵ A. Boveia¹¹⁹ J. Boyd³⁶ D. Boye²⁹ I. R. Boyko³⁸
J. Bracinik²⁰ N. Brahim^{62d} G. Brandt¹⁷¹ O. Brandt³² F. Braren⁴⁸ B. Brau¹⁰³ J. E. Brau¹²³ R. Brenner¹⁶⁹
L. Brenner¹¹⁴ R. Brenner¹⁶¹ S. Bressler¹⁶⁹ D. Britton⁵⁹ D. Britzger¹¹⁰ I. Brock²⁴ G. Brooijmans⁴¹
W. K. Brooks^{137f} E. Brost²⁹ L. M. Brown^{165j} L. E. Bruce⁶¹ T. L. Bruckler¹²⁶ P. A. Bruckman de Renstrom⁸⁷
B. Briuers⁴⁸ D. Bruncko^{28b,a} A. Bruni^{23b} G. Bruni^{23b} M. Bruschi^{23b} N. Bruscin^{75a,75b} T. Buanes¹⁶
Q. Buat¹³⁸ D. Buchin¹¹⁰ A. G. Buckley⁵⁹ M. K. Bugge¹²⁵ O. Bulekov³⁷ B. A. Bullard¹⁴³ S. Burdin⁹²
C. D. Burgard⁴⁹ A. M. Burger⁴⁰ B. Burghgrave⁸ O. Burlayenko⁵⁴ J. T. P. Burr³² C. D. Burton¹¹
J. C. Burzynski¹⁴² E. L. Busch⁴¹ V. Büscher¹⁰⁰ P. J. Bussey⁵⁹ J. M. Butler²⁵ C. M. Buttar⁵⁹
J. M. Butterworth⁹⁶ W. Buttinger¹³⁴ C. J. Buxo Vazquez¹⁰⁷ A. R. Buzykaev³⁷ S. Cabrera Urbán¹⁶³
L. Cadamuro⁶⁶ D. Caforio⁵⁸ H. Cai¹²⁹ Y. Cai^{14a,14e} V. M. M. Cairo³⁶ O. Cakir^{3a} N. Calace³⁶
P. Calafiura^{17a} G. Calderini¹²⁷ P. Calfayan⁶⁸ G. Callea⁵⁹ L. P. Caloba^{83b} D. Calvet⁴⁰ S. Calvet⁴⁰
T. P. Calvet¹⁰² M. Calvetti^{74a,74b} R. Camacho Toro¹²⁷ S. Camarda³⁶ D. Camarero Munoz²⁶ P. Camarri^{76a,76b}
M. T. Camerlingo^{72a,72b} D. Cameron¹²⁵ C. Camincher¹⁶⁵ M. Campanelli⁹⁶ A. Camplani⁴² V. Canale^{72a,72b}
A. Canesse¹⁰⁴ M. Cano Bret⁸⁰ J. Cantero¹⁶³ Y. Cao¹⁶² F. Capocasa²⁶ M. Capua^{43b,43a} A. Carbone^{71a,71b}
R. Cardarelli^{76a} J. C. J. Cardenas⁸ F. Cardillo¹⁶³ T. Carli³⁶ G. Carlino^{72a} J. I. Carlotto¹³ B. T. Carlson^{129,k}
E. M. Carlson^{165,156a} L. Carminati^{71a,71b} A. Carnelli¹³⁵ M. Carnesale^{75a,75b} S. Caron¹¹³ E. Carquin^{137f}
S. Carrá^{71a,71b} G. Carratta^{23b,23a} F. Carrio Argos^{33g} J. W. S. Carter¹⁵⁵ T. M. Carter⁵² M. P. Casado^{13,1}
M. Caspar⁴⁸ E. G. Castiglia¹⁷² F. L. Castillo⁴ L. Castillo Garcia¹³ V. Castillo Gimenez¹⁶³ N. F. Castro^{130a,130e}
A. Catinaccio³⁶ J. R. Catmore¹²⁵ V. Cavaliere²⁹ N. Cavalli^{23b,23a} V. Cavalasini^{74a,74b} Y. C. Cekmecelioglu⁴⁸
E. Celebi^{21a} F. Celli¹²⁶ M. S. Centonze^{70a,70b} K. Cerny¹²² A. S. Cerqueira^{83a} A. Cerri¹⁴⁶ L. Cerrito^{76a,76b}
F. Cerutti^{17a} B. Cervato¹⁴¹ A. Cervelli^{23b} G. Cesarini⁵³ S. A. Cetin⁸² Z. Chadi^{35a} D. Chakraborty¹¹⁵
M. Chala^{130f} J. Chan¹⁷⁰ W. Y. Chan¹⁵³ J. D. Chapman³² E. Chapon¹³⁵ B. Chargeishvili^{149b} D. G. Charlton²⁰
T. P. Charman⁹⁴ M. Chatterjee¹⁹ C. Chauhan¹³³ S. Chekanov⁶ S. V. Chekulaev^{156a} G. A. Chelkov^{38,m}
A. Chen¹⁰⁶ B. Chen¹⁵¹ B. Chen¹⁶⁵ H. Chen^{14c} H. Chen²⁹ J. Chen^{62c} J. Chen¹⁴² M. Chen¹²⁶ S. Chen¹⁵³
S. J. Chen^{14c} X. Chen^{62c,135} X. Chen^{14b,n} Y. Chen^{62a} C. L. Cheng¹⁷⁰ H. C. Cheng^{64a} S. Cheong¹⁴³
A. Cheplakov³⁸ E. Cheremushkina⁴⁸ E. Cherepanova¹¹⁴ R. Cherkaoui El Moursli^{35e} E. Cheu⁷ K. Cheung⁶⁵
L. Chevalier¹³⁵ V. Chiarella⁵³ G. Chiarelli^{74a} N. Chiedde¹⁰² G. Chiodini^{70a} A. S. Chisholm²⁰ A. Chitan^{27b}
M. Chitishvili¹⁶³ M. V. Chizhov³⁸ K. Choi¹¹ A. R. Chomont^{75a,75b} Y. Chou¹⁰³ E. Y. S. Chow¹¹⁴
T. Chowdhury^{33g} K. L. Chu¹⁶⁹ M. C. Chu^{64a} X. Chu^{14a,14e} J. Chudoba¹³¹ J. J. Chwastowski⁸⁷ D. Cieri¹¹⁰
K. M. Ciesla^{86a} V. Cindro⁹³ A. Ciocio^{17a} F. Ciroto^{72a,72b} Z. H. Citron^{169,o} M. Citterio^{71a} D. A. Ciubotaru^{27b}
B. M. Ciungu¹⁵⁵ A. Clark⁵⁶ P. J. Clark⁵² J. M. Clavijo⁴⁸ S. E. Clawson⁴⁸ C. Clement^{47a,47b}
J. Clercx⁴⁸ L. Clissa^{23b,23a} Y. Coadou¹⁰² M. Cobal^{69a,69c} A. Coccaro^{57b} R. F. Coelho Barrue^{130a}
R. Coelho Lopes De Sa¹⁰³ S. Coelli^{71a} H. Cohen¹⁵¹ A. E. C. Coimbra^{71a,71b} B. Cole⁴¹ J. Collot⁶⁰
P. Conde Muñoa^{130a,130g} M. P. Connell^{33c} S. H. Connell^{33c} I. A. Connelly⁵⁹ E. I. Conroy¹²⁶ F. Conventi^{72a,p}
H. G. Cooke²⁰ A. M. Cooper-Sarkar¹²⁶ A. Cordeiro Oudot Choi¹²⁷ F. Cormier¹⁶⁴ L. D. Corpe⁴⁰
M. Corradi^{75a,75b} F. Corriveau^{104,q} A. Cortes-Gonzalez¹⁸ M. J. Costa¹⁶³ F. Costanza⁴ D. Costanzo¹³⁹
B. M. Cote¹¹⁹ G. Cowan⁹⁵ K. Cranmer¹⁷⁰ D. Cremonini^{23b,23a} S. Crépe-Renaudin⁶⁰ F. Crescioli¹²⁷
M. Cristinziani¹⁴¹ M. Cristoforetti^{78a,78b} V. Croft¹¹⁴ J. E. Crosby¹²¹ G. Crosetti^{43b,43a} A. Cueto⁹⁹
T. Cuhadar Donszelmann¹⁶⁰ H. Cui^{14a,14e} Z. Cui⁷ W. R. Cunningham⁵⁹ F. Curcio^{43b,43a} P. Czodrowski³⁶

M. M. Czurylo^{63b} M. J. Da Cunha Sargedas De Sousa^{57b,57a} J. V. Da Fonseca Pinto^{83b} C. Da Via¹⁰¹
W. Dabrowski^{86a} T. Dado⁴⁹ S. Dahbi^{33g} T. Dai¹⁰⁶ D. Dal Santo¹⁹ C. Dallapiccola¹⁰³ M. Dam⁴²
G. D'amen²⁹ V. D'Amico¹⁰⁹ J. Damp¹⁰⁰ J. R. Dandoy¹²⁸ M. F. Daneri³⁰ M. Danninger¹⁴² V. Dao³⁶
G. Darbo^{57b} S. Darmora⁶ S. J. Das^{29,i} S. D'Auria^{71a,71b} C. David^{156b} T. Davidek¹³³ B. Davis-Purcell³⁴
I. Dawson⁹⁴ H. A. Day-hall¹³² K. De⁸ R. De Asmundis^{72a} N. De Biase⁴⁸ S. De Castro^{23b,23a} N. De Groot¹¹³
P. de Jong¹¹⁴ H. De la Torre¹⁰⁷ A. De Maria^{14c} A. De Salvo^{75a} U. De Sanctis^{76a,76b} A. De Santo¹⁴⁶
J. B. De Vivie De Regie⁶⁰ D. V. Dedovich³⁸ J. Degens¹¹⁴ A. M. Deiana⁴⁴ F. Del Corso^{23b,23a} J. Del Peso⁹⁹
F. Del Rio^{63a} F. Deliot¹³⁵ C. M. Delitzsch⁴⁹ M. Della Pietra^{72a,72b} D. Della Volpe⁵⁶ A. Dell'Acqua³⁶
L. Dell'Asta^{71a,71b} M. Delmastro⁴ P. A. Delsart⁶⁰ S. Demers¹⁷² M. Demichev³⁸ S. P. Denisov³⁷
L. D'Eramo⁴⁰ D. Derendarz⁸⁷ F. Derue¹²⁷ P. Dervan⁹² K. Desch²⁴ C. Deutsch²⁴ F. A. Di Bello^{57b,57a}
A. Di Ciaccio^{76a,76b} L. Di Ciaccio⁴ A. Di Domenico^{75a,75b} C. Di Donato^{72a,72b} A. Di Girolamo³⁶
G. Di Gregorio⁵ A. Di Luca^{78a,78b} B. Di Micco^{77a,77b} R. Di Nardo^{77a,77b} C. Diaconu¹⁰² M. Diamantopoulou³⁴
F. A. Dias¹¹⁴ T. Dias Do Vale¹⁴² M. A. Diaz^{137a,137b} F. G. Diaz Capriles²⁴ M. Didenko¹⁶³ E. B. Diehl¹⁰⁶
L. Diehl⁵⁴ S. Díez Cornell⁴⁸ C. Diez Pardos¹⁴¹ C. Dimitriadi^{161,24,161} A. Dimitrievska^{17a} J. Dingfelder²⁴
I-M. Dinu^{27b} S. J. Dittmeier^{63b} F. Dittus³⁶ F. Djama¹⁰² T. Djobava^{149b} J. I. Djuvsland¹⁶ C. Doglioni^{101,98}
J. Dolejsi¹³³ Z. Dolezal¹³³ M. Donadelli^{83c} B. Dong¹⁰⁷ J. Donini⁴⁰ A. D'Onofrio^{77a,77b} M. D'Onofrio⁹²
J. Dopke¹³⁴ A. Doria^{72a} N. Dos Santos Fernandes^{130a} M. T. Dova⁹⁰ A. T. Doyle⁵⁹ M. A. Draguet¹²⁶
E. Dreyer¹⁶⁹ I. Drivas-koulouris¹⁰ A. S. Drobac¹⁵⁸ M. Drozdova⁵⁶ D. Du^{62a} T. A. du Pree¹¹⁴ F. Dubinin³⁷
M. Dubovsky^{28a} E. Duchovni¹⁶⁹ G. Duckeck¹⁰⁹ O. A. Ducu^{27b} D. Duda⁵² A. Dudarev³⁶ E. R. Duden²⁶
M. D'uffizi¹⁰¹ L. Dufлот⁶⁶ M. Dührssen³⁶ C. Dülsen¹⁷¹ A. E. Dumitriu^{27b} M. Dunford^{63a} S. Dungs⁴⁹
K. Dunne^{47a,47b} A. Duperrin¹⁰² H. Duran Yildiz^{3a} M. Düren⁵⁸ A. Durglishvili^{149b} B. L. Dwyer¹¹⁵
G. I. Dyckes^{17a} M. Dyndal^{86a} S. Dysch¹⁰¹ B. S. Dziedzic⁸⁷ Z. O. Earnshaw¹⁴⁶ G. H. Eberwein¹²⁶
B. Eckerova^{28a} S. Eggebrecht⁵⁵ M. G. Eggleston⁵¹ E. Egidio Purcino De Souza¹²⁷ L. F. Ehrke⁵⁶ G. Eigen¹⁶
K. Einsweiler^{17a} T. Ekelof¹⁶¹ P. A. Ekman⁹⁸ S. El Farkh^{35b} Y. El Ghazali^{35b} H. El Jarrari^{35e,148}
A. El Moussaouy^{35a} V. Ellajosyula¹⁶¹ M. Ellert¹⁶¹ F. Ellinghaus¹⁷¹ A. A. Elliot⁹⁴ N. Ellis³⁶ J. Elmsheuser²⁹
M. Elsing³⁶ D. Emelianov¹³⁴ Y. Enari¹⁵³ I. Ene^{17a} S. Epari¹³ J. Erdmann⁴⁹ P. A. Erland⁸⁷ M. Errenst¹⁷¹
M. Escalier⁶⁶ C. Escobar¹⁶³ E. Etzion¹⁵¹ G. Evans^{130a} H. Evans⁶⁸ L. S. Evans⁹⁵ M. O. Evans¹⁴⁶
A. Ezhilov³⁷ S. Ezzarqtouni^{35a} F. Fabbri⁵⁹ L. Fabbri^{23b,23a} G. Facini⁹⁶ V. Fadeyev¹³⁶ R. M. Fakhruddinov³⁷
S. Falciano^{75a} L. F. Falda Ulhoa Coelho³⁶ P. J. Falke²⁴ J. Faltova¹³³ C. Fan¹⁶² Y. Fan^{14a} Y. Fang^{14a,14e}
M. Fanti^{71a,71b} M. Faraj^{69a,69b} Z. Farazpay⁹⁷ A. Farbin⁸ A. Farilla^{77a} T. Farooque¹⁰⁷ S. M. Farrington⁵²
F. Fassi^{35e} D. Fassouliotis⁹ M. Faucci Giannelli^{76a,76b} W. J. Fawcett³² L. Fayard⁶⁶ P. Federic¹³³
P. Federicova¹³¹ O. L. Fedin^{37,m} G. Fedotov³⁷ M. Feickert¹⁷⁰ L. Feligioni¹⁰² D. E. Fellers¹²³ C. Feng^{62b}
M. Feng^{14b} Z. Feng¹¹⁴ M. J. Fenton¹⁶⁰ A. B. Fenyuk³⁷ L. Ferencz⁴⁸ R. A. M. Ferguson⁹¹
S. I. Fernandez Luengo^{137f} M. J. V. Fernoux¹⁰² J. Ferrando⁴⁸ A. Ferrari¹⁶¹ P. Ferrari^{114,113} R. Ferrari^{73a}
D. Ferrere⁵⁶ C. Ferretti¹⁰⁶ F. Fiedler¹⁰⁰ A. Filipčič⁹³ E. K. Filmer¹ F. Filthaut¹¹³ M. C. N. Fiolhais^{130a,130c,r}
L. Fiorini¹⁶³ W. C. Fisher¹⁰⁷ T. Fitschen¹⁰¹ P. M. Fitzhugh¹³⁵ I. Fleck¹⁴¹ P. Fleischmann¹⁰⁶ T. Flick¹⁷¹
L. Flores¹²⁸ M. Flores^{33d,s} L. R. Flores Castillo^{64a} L. Flores Sanz De Acedo³⁶ F. M. Follega^{78a,78b} N. Fomin¹⁶
J. H. Foo¹⁵⁵ B. C. Forland⁶⁸ A. Formica¹³⁵ A. C. Forti¹⁰¹ E. Fortin³⁶ A. W. Fortman⁶¹ M. G. Foti^{17a}
L. Fountas^{9,t} D. Fournier⁶⁶ H. Fox⁹¹ P. Francavilla^{74a,74b} S. Francescato⁶¹ S. Franchellucci⁵⁶
M. Franchini^{23b,23a} S. Franchino^{63a} D. Francis³⁶ L. Franco¹¹³ L. Franconi⁴⁸ M. Franklin⁶¹ G. Frattari²⁶
A. C. Freegard⁹⁴ W. S. Freund^{83b} Y. Y. Frid¹⁵¹ N. Fritzsche⁵⁰ A. Froch⁵⁴ D. Froidevaux³⁶ J. A. Frost¹²⁶
Y. Fu^{62a} M. Fujimoto¹¹⁸ E. Fullana Torregrosa^{163,a} K. Y. Fung^{64a} E. Furtado De Simas Filho^{83b}
M. Furukawa¹⁵³ J. Fuster¹⁶³ A. Gabrielli^{23b,23a} A. Gabrielli¹⁵⁵ P. Gadow³⁶ G. Gagliardi^{57b,57a}
L. G. Gagnon^{17a} E. J. Gallas¹²⁶ B. J. Gallop¹³⁴ K. K. Gan¹¹⁹ S. Ganguly¹⁵³ J. Gao^{62a} Y. Gao⁵²
F. M. Garay Walls^{137a,137b} B. Garcia^{29,i} C. García¹⁶³ A. Garcia Alonso¹¹⁴ A. G. Garcia Caffaro¹⁷²
J. E. García Navarro¹⁶³ M. Garcia-Sciveres^{17a} G. L. Gardner¹²⁸ R. W. Gardner³⁹ N. Garelli¹⁵⁸ D. Garg⁸⁰
R. B. Garg^{143,u} J. M. Gargan⁵² C. A. Garner¹⁵⁵ S. J. Gasiorowski¹³⁸ P. Gaspar^{83b} G. Gaudio^{73a} V. Gautam¹³
P. Gauzzi^{75a,75b} I. L. Gavrilenko³⁷ A. Gavrilyuk³⁷ C. Gay¹⁶⁴ G. Gaycken⁴⁸ E. N. Gazis¹⁰ A. A. Geanta^{27b}
C. M. Gee¹³⁶ C. Gemme^{57b} M. H. Genest⁶⁰ S. Gentile^{75a,75b} S. George⁹⁵ W. F. George²⁰ T. Gerialis⁴⁶

P. Gessinger-Befurt³⁶ M. E. Geyik¹⁷¹ M. Ghani¹⁶⁷ M. Ghneimat¹⁴¹ K. Ghorbanian⁹⁴ A. Ghosal¹⁴¹
 A. Ghosh¹⁶⁰ A. Ghosh⁷ B. Giacobbe^{23b} S. Giagu^{75a,75b} T. Giani¹¹⁴ P. Giannetti^{74a} A. Giannini^{62a}
 S. M. Gibson⁹⁵ M. Gignac¹³⁶ D. T. Gil^{86b} A. K. Gilbert^{86a} B. J. Gilbert⁴¹ D. Gillberg³⁴ G. Gilles¹¹⁴
 N. E. K. Gillwald⁴⁸ L. Ginabat¹²⁷ D. M. Gingrich^{2,e} M. P. Giordani^{69a,69c} P. F. Giraud¹³⁵ G. Giugliarelli^{69a,69c}
 D. Giugni^{71a} F. Giuli³⁶ I. Gkialas^{9,t} L. K. Gladilin³⁷ C. Glasman⁹⁹ G. R. Gledhill¹²³ G. Glemža⁴⁸
 M. Glisic¹²³ I. Gnesi^{43b,v} Y. Go^{29,i} M. Goblirsch-Kolb³⁶ B. Gocke⁴⁹ D. Godin¹⁰⁸ B. Gokturk^{21a}
 S. Goldfarb¹⁰⁵ T. Golling⁵⁶ M. G. D. Gololo^{33g} D. Golubkov³⁷ J. P. Gombas¹⁰⁷ A. Gomes^{130a,130b}
 G. Gomes Da Silva¹⁴¹ A. J. Gomez Delegido¹⁶³ R. Gonçalo^{130a,130c} G. Gonella¹²³ L. Gonella²⁰
 A. Gongadze^{149c} F. Gonnella²⁰ J. L. Gonski⁴¹ R. Y. González Andana⁵² S. González de la Hoz¹⁶³
 S. Gonzalez Fernandez¹³ R. Gonzalez Lopez⁹² C. Gonzalez Renteria^{17a} M. V. Gonzalez Rodrigues⁴⁸
 R. Gonzalez Suarez¹⁶¹ S. Gonzalez-Sevilla⁵⁶ G. R. Gonzalvo Rodriguez¹⁶³ L. Goossens³⁶ B. Gorini³⁶
 E. Gorini^{70a,70b} A. Gorišek⁹³ T. C. Gosart¹²⁸ A. T. Goshaw⁵¹ M. I. Gostkin³⁸ S. Goswami¹²¹
 C. A. Gottardo³⁶ S. A. Gotz¹⁰⁹ M. Goughri^{35b} V. Goumarre⁴⁸ A. G. Goussiou¹³⁸ N. Govender^{33c}
 I. Grabowska-Bold^{86a} K. Graham³⁴ E. Gramstad¹²⁵ S. Grancagnolo^{70a,70b} M. Grandi¹⁴⁶ P. M. Gravila^{27f}
 F. G. Gravili^{70a,70b} H. M. Gray^{17a} M. Greco^{70a,70b} C. Greife²⁴ I. M. Gregor⁴⁸ P. Grenier¹⁴³ C. Grieco¹³
 A. A. Grillo¹³⁶ K. Grimm³¹ S. Grinstein^{13,w} J.-F. Grivaz⁶⁶ E. Gross¹⁶⁹ J. Grosse-Knetter⁵⁵ C. Grud¹⁰⁶
 J. C. Grundy¹²⁶ L. Guan¹⁰⁶ W. Guan²⁹ C. Gubbels¹⁶⁴ J. G. R. Guerrero Rojas¹⁶³ G. Guerrieri^{69a,69c}
 F. Guescini¹¹⁰ R. Gugel¹⁰⁰ J. A. M. Guhit¹⁰⁶ A. Guida¹⁸ T. Guillemain⁴ E. Guillon^{167,134} S. Guindon³⁶
 F. Guo^{14a,14e} J. Guo^{62c} L. Guo⁴⁸ Y. Guo¹⁰⁶ R. Gupta⁴⁸ S. Gurbuz²⁴ S. S. Gurdasani⁵⁴ G. Gustavino³⁶
 M. Guth⁵⁶ P. Gutierrez¹²⁰ L. F. Gutierrez Zagazeta¹²⁸ C. Gutschow⁹⁶ C. Gwenlan¹²⁶ C. B. Gwilliam⁹²
 E. S. Haaland¹²⁵ A. Haas¹¹⁷ M. Habedank⁴⁸ C. Haber^{17a} H. K. Hadavand⁸ A. Hadeef¹⁰⁰ S. Hadzic¹¹⁰
 J. J. Hahn¹⁴¹ E. H. Haines⁹⁶ M. Haleem¹⁶⁶ J. Haley¹²¹ J. J. Hall¹³⁹ G. D. Hallewell¹⁰² L. Halser¹⁹
 K. Hamano¹⁶⁵ H. Hamdaoui^{35e} M. Hamer²⁴ G. N. Hamity⁵² E. J. Hampshire⁹⁵ J. Han^{62b} K. Han^{62a}
 L. Han^{14c} L. Han^{62a} S. Han^{17a} Y. F. Han¹⁵⁵ K. Hanagaki⁸⁴ M. Hance¹³⁶ D. A. Hangal^{41,d} H. Hanif¹⁴²
 M. D. Hank¹²⁸ R. Hankache¹⁰¹ J. B. Hansen⁴² J. D. Hansen⁴² P. H. Hansen⁴² K. Hara¹⁵⁷ D. Harada⁵⁶
 T. Harenberg¹⁷¹ S. Harkusha³⁷ M. L. Harris¹⁰³ Y. T. Harris¹²⁶ J. Harrison¹³ N. M. Harrison¹¹⁹
 P. F. Harrison¹⁶⁷ N. M. Hartman¹¹⁰ N. M. Hartmann¹⁰⁹ Y. Hasegawa¹⁴⁰ A. Hasib⁵² S. Haug¹⁹ R. Hauser¹⁰⁷
 C. M. Hawkes²⁰ R. J. Hawkins³⁶ Y. Hayashi¹⁵³ S. Hayashida¹¹¹ D. Hayden¹⁰⁷ C. Hayes¹⁰⁶ R. L. Hayes¹¹⁴
 C. P. Hays¹²⁶ J. M. Hays⁹⁴ H. S. Hayward⁹² F. He^{62a} M. He^{14a,14e} Y. He¹⁵⁴ Y. He¹²⁷ N. B. Heatley⁹⁴
 V. Hedberg⁹⁸ A. L. Heggelund¹²⁵ N. D. Hehir⁹⁴ C. Heidegger⁵⁴ K. K. Heidegger⁵⁴ W. D. Heidorn⁸¹
 J. Heilman³⁴ S. Heim⁴⁸ T. Heim^{17a} J. G. Heinlein¹²⁸ J. J. Heinrich¹²³ L. Heinrich^{110,x} J. Hejbal¹³¹
 L. Helary⁴⁸ A. Held¹⁷⁰ S. Hellesund¹⁶ C. M. Helling¹⁶⁴ S. Hellman^{47a,47b} R. C. W. Henderson⁹¹
 L. Henkelmann³² A. M. Henriques Correia³⁶ H. Herde⁹⁸ Y. Hernández Jiménez¹⁴⁵ L. M. Herrmann²⁴
 T. Herrmann⁵⁰ G. Herten⁵⁴ R. Hertenberger¹⁰⁹ L. Hervas³⁶ M. E. Hespington¹⁰⁰ N. P. Hessey^{156a} H. Hibi⁸⁵
 S. J. Hillier²⁰ J. R. Hinds¹⁰⁷ F. Hinterkeuser²⁴ M. Hirose¹²⁴ S. Hirose¹⁵⁷ D. Hirschbuehl¹⁷¹
 T. G. Hitchings¹⁰¹ B. Hiti⁹³ J. Hobbs¹⁴⁵ R. Hobincu^{27e} N. Hod¹⁶⁹ M. C. Hodgkinson¹³⁹ B. H. Hodgkinson³²
 A. Hoecker³⁶ J. Hofer⁴⁸ T. Holm²⁴ M. Holzbock¹¹⁰ L. B. A. H. Hommels³² B. P. Honan¹⁰¹ J. Hong^{62c}
 T. M. Hong¹²⁹ B. H. Hooberman¹⁶² W. H. Hopkins⁶ Y. Horii¹¹¹ S. Hou¹⁴⁸ A. S. Howard⁹³ J. Howarth⁵⁹
 J. Hoya⁶ M. Hrabovsky¹²² A. Hrynevich⁴⁸ T. Hryn'ova⁴ P. J. Hsu⁶⁵ S.-C. Hsu¹³⁸ Q. Hu⁴¹ Y. F. Hu^{14a,14e}
 S. Huang^{64b} X. Huang^{14c} Y. Huang^{139,y} Y. Huang^{14a} Z. Huang¹⁰¹ Z. Hubacek¹³² M. Huebner²⁴
 F. Huegging²⁴ T. B. Huffman¹²⁶ C. A. Hugli⁴⁸ M. Huhtinen³⁶ S. K. Huiberts¹⁶ R. Hulsken¹⁰⁴
 N. Huseynov^{12,m} J. Huston¹⁰⁷ J. Huth⁶¹ R. Hyneman¹⁴³ G. Iacobucci⁵⁶ G. Iakovidis²⁹ I. Ibragimov¹⁴¹
 L. Iconomidou-Fayard⁶⁶ P. Iengo^{72a,72b} R. Iguchi¹⁵³ T. Iizawa⁸⁴ Y. Ikegami⁸⁴ N. Ilic¹⁵⁵ H. Imam^{35a}
 M. Ince Lezki⁵⁶ T. Ingebretsen Carlson^{47a,47b} G. Introzzi^{73a,73b} M. Iodice^{77a} V. Ippolito^{75a,75b} R. K. Irwin⁹²
 M. Ishino¹⁵³ W. Islam¹⁷⁰ C. Issever^{18,48} S. Istin^{21a,z} H. Ito¹⁶⁸ J. M. Iturbe Ponce^{64a} R. Iuppa^{78a,78b}
 A. Ivina¹⁶⁹ J. M. Izen⁴⁵ V. Izzo^{72a} P. Jacka^{131,132} P. Jackson¹ R. M. Jacobs⁴⁸ B. P. Jaeger¹⁴²
 C. S. Jagfeld¹⁰⁹ P. Jain⁵⁴ G. Jäkel¹⁷¹ K. Jakobs⁵⁴ T. Jakoubek¹⁶⁹ J. Jamieson⁵⁹ K. W. Janas^{86a}
 A. E. Jaspán⁹² M. Javurkova¹⁰³ F. Jeanneau¹³⁵ L. Jeanty¹²³ J. Jejelava^{149a,aa} P. Jenni^{54,bb} C. E. Jessiman³⁴
 S. Jézéquel⁴ C. Jia^{62b} J. Jia¹⁴⁵ X. Jia⁶¹ X. Jia^{14a,14e} Z. Jia^{14c} Y. Jiang^{62a} S. Jiggins⁴⁸ J. Jimenez Pena¹³

S. Jin^{14c} A. Jinaru^{27b} O. Jinnouchi¹⁵⁴ P. Johansson¹³⁹ K. A. Johns⁷ J. W. Johnson¹³⁶ D. M. Jones³²
 E. Jones⁴⁸ P. Jones³² R. W. L. Jones⁹¹ T. J. Jones⁹² R. Joshi¹¹⁹ J. Jovicevic¹⁵ X. Ju^{17a} J. J. Junggeburth³⁶
 T. Junkermann^{63a} A. Juste Rozas^{13,w} M. K. Juzek⁸⁷ S. Kabana^{137e} A. Kaczmarek⁸⁷ M. Kado¹¹⁰
 H. Kagan¹¹⁹ M. Kagan¹⁴³ A. Kahn⁴¹ A. Kahn¹²⁸ C. Kahra¹⁰⁰ T. Kaji¹⁶⁸ E. Kajomovitz¹⁵⁰ N. Kakati¹⁶⁹
 I. Kalaitzidou⁵⁴ C. W. Kalderon²⁹ A. Kamenshchikov¹⁵⁵ S. Kanayama¹⁵⁴ N. J. Kang¹³⁶ D. Kar^{33g}
 K. Karava¹²⁶ M. J. Kareem^{156b} E. Karentzos⁵⁴ I. Karkanas¹⁵² O. Karkout¹¹⁴ S. N. Karpov³⁸
 Z. M. Karpova³⁸ V. Kartvelishvili⁹¹ A. N. Karyukhin³⁷ E. Kasimi¹⁵² J. Katzy⁴⁸ S. Kaur³⁴ K. Kawade¹⁴⁰
 M. P. Kawale¹²⁰ T. Kawamoto¹³⁵ E. F. Kay³⁶ F. I. Kaya¹⁵⁸ S. Kazakos¹⁰⁷ V. F. Kazanin³⁷ Y. Ke¹⁴⁵
 J. M. Keaveney^{33a} R. Keeler¹⁶⁵ G. V. Kehris⁶¹ J. S. Keller³⁴ A. S. Kelly⁹⁶ J. J. Kempster¹⁴⁶ K. E. Kennedy⁴¹
 P. D. Kennedy¹⁰⁰ O. Kepka¹³¹ B. P. Kerridge¹⁶⁷ S. Kersten¹⁷¹ B. P. Kerševan⁹³ S. Keshri⁶⁶ L. Keszeghova^{28a}
 S. Ketabchi Haghighat¹⁵⁵ M. Khandoga¹²⁷ A. Khanov¹²¹ A. G. Kharlamov³⁷ T. Kharlamova³⁷ E. E. Khoda¹³⁸
 T. J. Khoo¹⁸ G. Khoriali¹⁶⁶ J. Khubua^{149b} Y. A. R. Khwaira⁶⁶ A. Kilgallon¹²³ D. W. Kim^{47a,47b} Y. K. Kim³⁹
 N. Kimura⁹⁶ A. Kirchhoff⁵⁵ C. Kirfel²⁴ F. Kirfel²⁴ J. Kirk¹³⁴ A. E. Kiryunin¹¹⁰ C. Kitsaki¹⁰
 O. Kivernyk²⁴ M. Klassen^{63a} C. Klein³⁴ L. Klein¹⁶⁶ M. H. Klein¹⁰⁶ M. Klein⁹² S. B. Klein⁵⁶ U. Klein⁹²
 P. Klimek³⁶ A. Klimentov²⁹ T. Klioutchnikova³⁶ P. Kluit¹¹⁴ S. Kluth¹¹⁰ E. Kneringer⁷⁹ T. M. Knight¹⁵⁵
 A. Kneue⁵⁴ R. Kobayashi⁸⁸ D. Kobylanski¹⁶⁹ S. F. Koch¹²⁶ M. Kocian¹⁴³ P. Kodyš¹³³ D. M. Koeck¹²³
 P. T. Koenig²⁴ T. Koffas³⁴ M. Kolb¹³⁵ I. Koletsou⁴ T. Komarek¹²² K. Köneke⁵⁴ A. X. Y. Kong¹
 T. Kono¹¹⁸ N. Konstantinidis⁹⁶ B. Konya⁹⁸ R. Kopeliānsky⁶⁸ S. Koperny^{86a} K. Korcyl⁸⁷ K. Kordas^{152,cc}
 G. Koren¹⁵¹ A. Korn⁹⁶ S. Korn⁵⁵ I. Korolkov¹³ N. Korotkova³⁷ B. Kortman¹¹⁴ O. Kortner¹¹⁰
 S. Kortner¹¹⁰ W. H. KostECKa¹¹⁵ V. V. Kostyukhin¹⁴¹ A. Kotskechagia¹³⁵ A. Kotwal⁵¹ A. Koulouris³⁶
 A. Kourkoumeli-Charalampidi^{73a,73b} C. Kourkoumelis⁹ E. Kourlitis^{110,x} O. Kovanda¹⁴⁶ R. Kowalewski¹⁶⁵
 W. Kozanecki¹³⁵ A. S. Kozhin³⁷ V. A. Kramarenko³⁷ G. Kramberger⁹³ P. Kramer¹⁰⁰ M. W. Krasny¹²⁷
 A. Krasznahorkay³⁶ J. W. Kraus¹⁷¹ J. A. Kremer¹⁰⁰ T. Kresse⁵⁰ J. Kretzschmar⁹² K. Kreul¹⁸ P. Krieger¹⁵⁵
 S. Krishnamurthy¹⁰³ M. Krivos¹³³ K. Krizka²⁰ K. Kroeninger⁴⁹ H. Kroha¹¹⁰ J. Kroll¹³¹ J. Kroll¹²⁸
 K. S. Krowpman¹⁰⁷ U. Kruchonak³⁸ H. Krüger²⁴ N. Krumnack⁸¹ M. C. Kruse⁵¹ J. A. Krzysiak⁸⁷
 O. Kuchinskaia³⁷ S. Kuday^{3a} S. Kuehn³⁶ R. Kuesters⁵⁴ T. Kuhl⁴⁸ V. Kukhtin³⁸ Y. Kulchitsky^{37,m}
 S. Kuleshov^{137d,137b} M. Kumar^{33g} N. Kumari⁴⁸ A. Kupco¹³¹ T. Kupfer⁴⁹ A. Kupich³⁷ O. Kuprash⁵⁴
 H. Kurashige⁸⁵ L. L. Kurchaninov^{156a} O. Kurdysh⁶⁶ Y. A. Kurochkin³⁷ A. Kurova³⁷ M. Kuze¹⁵⁴
 A. K. Kvam¹⁰³ J. Kvita¹²² T. Kwan¹⁰⁴ N. G. Kyriacou¹⁰⁶ L. A. O. Laatu¹⁰² C. Lacasta¹⁶³ F. Lacava^{75a,75b}
 H. Lacker¹⁸ D. Lacour¹²⁷ N. N. Lad⁹⁶ E. Ladygin³⁸ B. Laforge¹²⁷ T. Lagouri^{137e} S. Lai⁵⁵
 I. K. Lakomic^{86a} N. Lalloue⁶⁰ J. E. Lambert^{165,j} S. Lammers⁶⁸ W. Lampl⁷ C. Lampoudis^{152,cc}
 A. N. Lancaster¹¹⁵ E. Lançon²⁹ U. Landgraf⁵⁴ M. P. J. Landon⁹⁴ V. S. Lang⁵⁴ R. J. Langenberg¹⁰³
 O. K. B. Langrekken¹²⁵ A. J. Lankford¹⁶⁰ F. Lanni³⁶ K. Lantzsch²⁴ A. Lanza^{73a} A. Lapertosa^{57b,57a}
 J. F. Laporte¹³⁵ T. Lari^{71a} F. Lasagni Manghi^{23b} M. Lassnig³⁶ V. Latonova¹³¹ A. Laudrain¹⁰⁰ A. Laurier¹⁵⁰
 S. D. Lawlor⁹⁵ Z. Lawrence¹⁰¹ M. Lazzaroni^{71a,71b} B. Le¹⁰¹ E. M. Le Boulicaut⁵¹ B. Leban⁹³ A. Lebedev⁸¹
 M. LeBlanc³⁶ F. Ledroit-Guillon⁶⁰ A. C. A. Lee⁹⁶ S. C. Lee¹⁴⁸ S. Lee^{47a,47b} T. F. Lee⁹² L. L. Leeuw^{33c}
 H. P. Lefebvre⁹⁵ M. Lefebvre¹⁶⁵ C. Leggett^{17a} G. Lehmann Miotto³⁶ M. Leigh⁵⁶ W. A. Leight¹⁰³
 W. Leinonen¹¹³ A. Leisos^{152,dd} M. A. L. Leite^{83c} C. E. Leitgeb⁴⁸ R. Leitner¹³³ K. J. C. Leney⁴⁴ T. Lenz²⁴
 S. Leone^{74a} C. Leonidopoulos⁵² A. Leopold¹⁴⁴ C. Leroy¹⁰⁸ R. Les¹⁰⁷ C. G. Lester³² M. Levchenko³⁷
 J. Levêque⁴ D. Levin¹⁰⁶ L. J. Levinson¹⁶⁹ M. P. Lewicki⁸⁷ D. J. Lewis⁴ A. Li⁵ B. Li^{62b} C. Li^{62a} C-Q. Li^{62c}
 H. Li^{62a} H. Li^{62b} H. Li^{14c} H. Li^{62b} K. Li¹³⁸ L. Li^{62c} M. Li^{14a,14e} Q. Y. Li^{62a} S. Li^{14a,14e} S. Li^{62d,62c,ee}
 T. Li^{5,ff} X. Li¹⁰⁴ Z. Li¹²⁶ Z. Li¹⁰⁴ Z. Li⁹² Z. Li^{14a,14e} S. Liang^{14a,14e} Z. Liang^{14a} M. Liberatore^{135,gg}
 B. Liberti^{76a} K. Lieber^{64c} J. Lieber Marin^{83b} H. Lien⁶⁸ K. Lin¹⁰⁷ R. E. Lindley⁷ J. H. Lindon² E. Lipeles¹²⁸
 A. Lipniacka¹⁶ A. Lister¹⁶⁴ J. D. Little⁴ B. Liu^{14a} B. X. Liu¹⁴² D. Liu^{62d,62c} J. B. Liu^{62a} J. K. K. Liu³²
 K. Liu^{62d,62c} M. Liu^{62a} M. Y. Liu^{62a} P. Liu^{14a} Q. Liu^{62d,138,62c} X. Liu^{62a} Y. Liu^{14d,14e} Y. L. Liu^{62b}
 Y. W. Liu^{62a} J. Llorente Merino¹⁴² S. L. Lloyd⁹⁴ E. M. Lobodzinska⁴⁸ P. Loch⁷ S. Loffredo^{76a,76b} T. Lohse¹⁸
 K. Lohwasser¹³⁹ E. Loiacono⁴⁸ M. Lokajicek^{131,a} J. D. Lomas²⁰ J. D. Long¹⁶² I. Longarini¹⁶⁰
 L. Longo^{70a,70b} R. Longo¹⁶² I. Lopez Paz⁶⁷ A. Lopez Solis⁴⁸ J. Lorenz¹⁰⁹ N. Lorenzo Martinez⁴
 A. M. Lory¹⁰⁹ O. Loseva³⁷ X. Lou^{47a,47b} X. Lou^{14a,14e} A. Lounis⁶⁶ J. Love⁶ P. A. Love⁹¹ G. Lu^{14a,14e}

M. Lu⁸⁰, S. Lu¹²⁸, Y. J. Lu⁶⁵, H. J. Lubatti¹³⁸, C. Luci^{75a,75b}, F. L. Lucio Alves^{14c}, A. Lucotte⁶⁰, F. Luehring⁶⁸,
 I. Luise¹⁴⁵, O. Lukianchuk⁶⁶, O. Lundberg¹⁴⁴, B. Lund-Jensen¹⁴⁴, N. A. Luongo¹²³, M. S. Lutz¹⁵¹, D. Lynn²⁹,
 H. Lyons⁹², R. Lysak¹³¹, E. Lytken⁹⁸, V. Lyubushkin³⁸, T. Lyubushkina³⁸, M. M. Lyukova¹⁴⁵, H. Ma²⁹, K. Ma^{62a},
 L. L. Ma^{62b}, Y. Ma¹²¹, D. M. Mac Donnell¹⁶⁵, G. Maccarrone⁵³, J. C. MacDonald¹⁰⁰, R. Madar⁴⁰, W. F. Mader⁵⁰,
 J. Maeda⁸⁵, T. Maeno²⁹, M. Maerker⁵⁰, H. Maguire¹³⁹, V. Maiboroda¹³⁵, A. Maio^{130a,130b,130d}, K. Maj^{86a},
 O. Majersky⁴⁸, S. Majewski¹²³, N. Makovec⁶⁶, V. Maksimovic¹⁵, B. Malaescu¹²⁷, Pa. Malecki⁸⁷,
 V. P. Maleev³⁷, F. Malek⁶⁰, M. Mali⁹³, D. Malito^{95,hh}, U. Mallik⁸⁰, S. Maltezos¹⁰, S. Malyukov³⁸, J. Mamuzic¹³,
 G. Mancini⁵³, G. Manco^{73a,73b}, J. P. Mandalia⁹⁴, I. Mandić⁹³, L. Manhaes de Andrade Filho^{83a}, I. M. Maniatis¹⁶⁹,
 J. Manjarres Ramos^{102,ii}, D. C. Mankad¹⁶⁹, A. Mann¹⁰⁹, B. Mansoulie¹³⁵, S. Manzoni³⁶, A. Marantis^{152,dd},
 G. Marchiori⁵, M. Marcisovsky¹³¹, C. Marcon^{71a,71b}, M. Marinescu²⁰, M. Marjanovic¹²⁰, E. J. Marshall⁹¹,
 Z. Marshall^{17a}, S. Marti-Garcia¹⁶³, T. A. Martin¹⁶⁷, V. J. Martin⁵², B. Martin dit Latour¹⁶, L. Martinelli^{75a,75b},
 M. Martinez^{13,w}, P. Martinez Agullo¹⁶³, V. I. Martinez Outschoorn¹⁰³, P. Martinez Suarez¹³, S. Martin-Haugh¹³⁴,
 V. S. Martoiu^{27b}, A. C. Martyniuk⁹⁶, A. Marzin³⁶, D. Mascione^{78a,78b}, L. Masetti¹⁰⁰, T. Mashimo¹⁵³, J. Masik¹⁰¹,
 A. L. Maslennikov³⁷, L. Massa^{23b}, P. Massarotti^{72a,72b}, P. Mastrandrea^{74a,74b}, A. Mastroberardino^{43b,43a},
 T. Masubuchi¹⁵³, T. Mathisen¹⁶¹, J. Matousek¹³³, N. Matsuzawa¹⁵³, J. Maurer^{27b}, B. Maček⁹³, D. A. Maximov³⁷,
 R. Mazini¹⁴⁸, I. Maznas¹⁵², M. Mazza¹⁰⁷, S. M. Mazza¹³⁶, E. Mazzeo^{71a,71b}, C. Mc Ginn²⁹, J. P. Mc Gowan¹⁰⁴,
 S. P. Mc Kee¹⁰⁶, E. F. McDonald¹⁰⁵, A. E. McDougall¹¹⁴, J. A. Mcfayden¹⁴⁶, R. P. McGovern¹²⁸,
 G. Mchedlidze^{149b}, R. P. McKenzie^{33g}, T. C. McLachlan⁴⁸, D. J. McLaughlin⁹⁶, K. D. McLean¹⁶⁵,
 S. J. McMahon¹³⁴, P. C. McNamara¹⁰⁵, C. M. Mcpartland⁹², R. A. McPherson^{165,q}, S. Mehlhase¹⁰⁹, A. Mehta⁹²,
 D. Melini¹⁵⁰, B. R. Mellado Garcia^{33g}, A. H. Melo⁵⁵, F. Meloni⁴⁸, A. M. Mendes Jacques Da Costa¹⁰¹,
 H. Y. Meng¹⁵⁵, L. Meng⁹¹, S. Menke¹¹⁰, M. Mentink³⁶, E. Meoni^{43b,43a}, C. Merlassino¹²⁶, L. Merola^{72a,72b},
 C. Meroni^{71a,71b}, G. Merz¹⁰⁶, O. Meshkov³⁷, J. Metcalfe⁶, A. S. Mete⁶, C. Meyer⁶⁸, J-P. Meyer¹³⁵,
 R. P. Middleton¹³⁴, L. Mijović⁵², G. Mikenberg¹⁶⁹, M. Mikesstikova¹³¹, M. Mikuž⁹³, H. Mildner¹⁰⁰, A. Milic³⁶,
 C. D. Milke⁴⁴, D. W. Miller³⁹, L. S. Miller³⁴, A. Milov¹⁶⁹, D. A. Milstead^{47a,47b}, T. Min^{14c}, A. A. Minaenko³⁷,
 I. A. Minashvili^{149b}, L. Mince⁵⁹, A. I. Mincer¹¹⁷, B. Mindur^{86a}, M. Mineev³⁸, Y. Mino⁸⁸, L. M. Mir¹³,
 M. Miralles Lopez¹⁶³, M. Mironova^{17a}, A. Mishima¹⁵³, M. C. Missio¹¹³, T. Mitani¹⁶⁸, A. Mitra¹⁶⁷,
 V. A. Mitsou¹⁶³, O. Miu¹⁵⁵, P. S. Miyagawa⁹⁴, Y. Miyazaki⁸⁹, A. Mizukami⁸⁴, T. Mkrtchyan^{63a}, M. Mlinarevic⁹⁶,
 T. Mlinarevic⁹⁶, M. Mlynarikova³⁶, S. Mobius¹⁹, K. Mochizuki¹⁰⁸, P. Moder⁴⁸, P. Mogg¹⁰⁹,
 A. F. Mohammed^{14a,14e}, S. Mohapatra⁴¹, G. Mokgatitwane^{33g}, L. Moleri¹⁶⁹, B. Mondal¹⁴¹, S. Mondal¹³²,
 G. Monig¹⁴⁶, K. Mönig⁴⁸, E. Monnier¹⁰², L. Monsonis Romero¹⁶³, J. Montejo Berlingen^{13,84}, M. Montella¹¹⁹,
 F. Montekali^{77a,77b}, F. Monticelli⁹⁰, S. Monzani^{69a,69c}, N. Morange⁶⁶, A. L. Moreira De Carvalho^{130a},
 M. Moreno Llácer¹⁶³, C. Moreno Martinez⁵⁶, P. Morettini^{57b}, S. Morgenstern³⁶, M. Morii⁶¹, M. Morinaga¹⁵³,
 A. K. Morley³⁶, F. Morodei^{75a,75b}, L. Morvaj³⁶, P. Moschovakos³⁶, B. Moser³⁶, M. Mosidze^{149b}, T. Moskalets⁵⁴,
 P. Moskvitina¹¹³, J. Moss^{31,ij}, E. J. W. Moyse¹⁰³, O. Mtintsilana^{33g}, S. Muanza¹⁰², J. Mueller¹²⁹,
 D. Muenstermann⁹¹, R. Müller¹⁹, G. A. Mullier¹⁶¹, A. J. Mullin³², J. J. Mullin¹²⁸, D. P. Mungo¹⁵⁵,
 D. Munoz Perez¹⁶³, F. J. Munoz Sanchez¹⁰¹, M. Murin¹⁰¹, W. J. Murray^{167,134}, A. Murrone^{71a,71b}, J. M. Muse¹²⁰,
 M. Muškinja^{17a}, C. Mwewa²⁹, A. G. Myagkov^{37,m}, A. J. Myers⁸, A. A. Myers¹²⁹, G. Myers⁶⁸, M. Myska¹³²,
 B. P. Nachman^{17a}, O. Nackenhorst⁴⁹, A. Nag⁵⁰, K. Nagai¹²⁶, K. Nagano⁸⁴, J. L. Nagle^{29,i}, E. Nagy¹⁰²,
 A. M. Nairz³⁶, Y. Nakahama⁸⁴, K. Nakamura⁸⁴, K. Nakkalil⁵, H. Nanjo¹²⁴, R. Narayan⁴⁴, E. A. Narayanan¹¹²,
 I. Naryshkin³⁷, M. Naseri³⁴, S. Nasri¹⁵⁹, C. Nass²⁴, G. Navarro^{22a}, J. Navarro-Gonzalez¹⁶³, R. Nayak¹⁵¹,
 A. Nayaz¹⁸, P. Y. Nechaeva³⁷, F. Nechansky⁴⁸, L. Nedic¹²⁶, T. J. Neep²⁰, A. Negri^{73a,73b}, M. Negrini^{23b},
 C. Nellist¹¹⁴, C. Nelson¹⁰⁴, K. Nelson¹⁰⁶, S. Nemecek¹³¹, M. Nessi^{36,kk}, M. S. Neubauer¹⁶², F. Neuhaus¹⁰⁰,
 J. Neundorff⁴⁸, R. Newhouse¹⁶⁴, P. R. Newman²⁰, C. W. Ng¹²⁹, Y. W. Y. Ng⁴⁸, B. Ngair^{35e}, H. D. N. Nguyen¹⁰⁸,
 R. B. Nickerson¹²⁶, R. Nicolaidou¹³⁵, J. Nielsen¹³⁶, M. Niemeyer⁵⁵, J. Niermann^{55,36}, N. Nikiforou³⁶,
 V. Nikolaenko^{37,m}, I. Nikolic-Audit¹²⁷, K. Nikolopoulos²⁰, P. Nilsson²⁹, I. Ninca⁴⁸, H. R. Nindhito⁵⁶,
 G. Ninio¹⁵¹, A. Nisati^{75a}, N. Nishu², R. Nisius¹¹⁰, J-E. Nitschke⁵⁰, E. K. Nkadimeng^{33g}, S. J. Noacco Rosende⁹⁰,
 T. Nobe¹⁵³, D. L. Noel³², T. Nommensen¹⁴⁷, M. B. Norfolk¹³⁹, R. R. B. Norisam⁹⁶, B. J. Norman³⁴, J. Novak⁹³,
 T. Novak⁴⁸, L. Novotny¹³², R. Novotny¹¹², L. Nozka¹²², K. Ntekas¹⁶⁰, N. M. J. Nunes De Moura Junior^{83b},
 E. Nurse⁹⁶, J. Ocariz¹²⁷, A. Ochi⁸⁵, I. Ochoa^{130a}, S. Oerdek^{48,ll}, J. T. Offermann³⁹, A. Ogrodnik¹³³, A. Oh¹⁰¹

C. C. Ohm¹⁴⁴ H. Oide⁸⁴ R. Oishi¹⁵³ M. L. Ojeda⁴⁸ Y. Okazaki⁸⁸ M. W. O'Keefe⁹² Y. Okumura¹⁵³
L. F. Oleiro Seabra^{130a} S. A. Olivares Pino^{137d} D. Oliveira Damazio²⁹ D. Oliveira Goncalves^{83a} J. L. Oliver¹⁶⁰
A. Olszewski⁸⁷ Ö. O. Öncel⁵⁴ D. C. O'Neil¹⁴² A. P. O'Neill¹⁹ A. Onofre^{130a,130e} P. U. E. Onyisi¹¹
M. J. Oreglia³⁹ G. E. Orellana⁹⁰ D. Orestano^{77a,77b} N. Orlando¹³ R. S. Orr¹⁵⁵ V. O'Shea⁵⁹ L. M. Osojnak¹²⁸
R. Ospanov^{62a} G. Otero y Garzon³⁰ H. Otono⁸⁹ P. S. Ott^{63a} G. J. Ottino^{17a} M. Ouchrif^{35d} J. Ouellette²⁹
F. Ould-Saada¹²⁵ M. Owen⁵⁹ R. E. Owen¹³⁴ K. Y. Oyulmaz^{21a} V. E. Ozcan^{21a} N. Ozturk⁸ S. Ozturk⁸²
H. A. Pacey³² A. Pacheco Pages¹³ C. Padilla Aranda¹³ G. Padovano^{75a,75b} S. Pagan Griso^{17a} G. Palacino⁶⁸
A. Palazzo^{70a,70b} S. Palestini³⁶ J. Pan¹⁷² T. Pan^{64a} D. K. Panchal¹¹ C. E. Pandini¹¹⁴ J. G. Panduro Vazquez⁹⁵
H. D. Pandya¹ H. Pang^{14b} P. Pani⁴⁸ G. Panizzo^{69a,69c} L. Paolozzi⁵⁶ C. Papadatos¹⁰⁸ S. Parajuli⁴⁴
A. Paramonov⁶ C. Paraskevopoulos¹⁰ D. Paredes Hernandez^{64b} T. H. Park¹⁵⁵ M. A. Parker³² F. Parodi^{57b,57a}
E. W. Parrish¹¹⁵ V. A. Parrish⁵² J. A. Parsons⁴¹ U. Parzefall⁵⁴ B. Pascual Dias¹⁰⁸ L. Pascual Dominguez¹⁵¹
F. Pasquali¹¹⁴ E. Pasqualucci^{75a} S. Passaggio^{57b} F. Pastore⁹⁵ P. Pasuwan^{47a,47b} P. Patel⁸⁷ U. M. Patel⁵¹
J. R. Pater¹⁰¹ T. Pauly³⁶ J. Pearkes¹⁴³ M. Pedersen¹²⁵ R. Pedro^{130a} S. V. Peleganchuk³⁷ O. Penc³⁶
E. A. Pender⁵² H. Peng^{62a} K. E. Pensi¹⁰⁹ M. Penzin³⁷ B. S. Peralva^{83d} A. P. Pereira Peixoto⁶⁰
L. Pereira Sanchez^{47a,47b} D. V. Perepelitsa^{29,i} E. Perez Codina^{156a} M. Perganti¹⁰ L. Perini^{71a,71b,a}
H. Pernegger³⁶ O. Perrin⁴⁰ K. Peters⁴⁸ R. F. Y. Peters¹⁰¹ B. A. Petersen³⁶ T. C. Petersen⁴² E. Petit¹⁰²
V. Petousis¹³² C. Petridou^{152,cc} A. Petrukhin¹⁴¹ M. Pettee^{17a} N. E. Pettersson³⁶ A. Petukhov³⁷
K. Petukhova¹³³ A. Peyaud¹³⁵ R. Pezoa^{137f} L. Pezzotti³⁶ G. Pezzullo¹⁷² T. M. Pham¹⁷⁰ T. Pham¹⁰⁵
P. W. Phillips¹³⁴ G. Piacquadio¹⁴⁵ E. Pianori^{17a} F. Piazza^{71a,71b} R. Piegai³⁰ D. Pietreanu^{27b}
A. D. Pilkington¹⁰¹ M. Pinamonti^{69a,69c} J. L. Pinfold² B. C. Pinheiro Pereira^{130a} A. E. Pinto Pinoargote¹³⁵
L. Pintucci^{69a,69c} K. M. Piper¹⁴⁶ A. Pirttikoski⁵⁶ C. Pitman Donaldson⁹⁶ D. A. Pizzi³⁴ L. Pizzimento^{64b}
A. Pizzini¹¹⁴ M.-A. Pleier²⁹ V. Plesanovs⁵⁴ V. Pleskot¹³³ E. Plotnikova³⁸ G. Poddar⁴ R. Poettgen⁹⁸
L. Poggioli¹²⁷ I. Pokharel⁵⁵ S. Polacek¹³³ G. Polesello^{73a} A. Poley^{142,156a} R. Polifka¹³² A. Polini^{23b}
C. S. Pollard¹⁶⁷ Z. B. Pollock¹¹⁹ V. Polychronakos²⁹ E. Pompa Pacchi^{75a,75b} D. Ponomarenko¹¹³
L. Pontecorvo³⁶ S. Popa^{27a} G. A. Popeneciu^{27d} A. Poreba³⁶ D. M. Portillo Quintero^{156a} S. Pospisil¹³²
M. A. Postill¹³⁹ P. Postolache^{27c} K. Potamianos¹⁶⁷ P. A. Potepa^{86a} I. N. Potrap³⁸ C. J. Potter³² H. Potti¹
T. Poulsen⁴⁸ J. Poveda¹⁶³ M. E. Pozo Astigarraga³⁶ A. Prades Ibanez¹⁶³ J. Pretel⁵⁴ D. Price¹⁰¹
M. Primavera^{70a} M. A. Principe Martin⁹⁹ R. Privara¹²² T. Procter⁵⁹ M. L. Proffitt¹³⁸ N. Proklova¹²⁸
K. Prokofiev^{64c} G. Proto¹¹⁰ S. Protopopescu²⁹ J. Proudfoot⁶ M. Przybycien^{86a} W. W. Przygoda^{86b}
J. E. Puddefoot¹³⁹ D. Pudzha³⁷ D. Pyatizbyantseva³⁷ J. Qian¹⁰⁶ D. Qichen¹⁰¹ Y. Qin¹⁰¹ T. Qiu⁵²
A. Quadt⁵⁵ M. Queitsch-Maitland¹⁰¹ G. Quetant⁵⁶ R. P. Quinn¹⁶⁴ G. Rabanal Bolanos⁶¹ D. Rafanoharana⁵⁴
F. Ragusa^{71a,71b} J. L. Rainbolt³⁹ J. A. Raine⁵⁶ S. Rajagopalan²⁹ E. Ramakoti³⁷ K. Ran^{48,14e}
N. P. Rapheeha^{33g} H. Rasheed^{27b} V. Raskina¹²⁷ D. F. Rassloff^{63a} S. Rave¹⁰⁰ B. Ravina⁵⁵ I. Ravinovich¹⁶⁹
M. Raymond³⁶ A. L. Read¹²⁵ N. P. Readioff¹³⁹ D. M. Rebutti^{73a,73b} G. Redlinger²⁹ A. S. Reed¹¹⁰
K. Reeves²⁶ J. A. Reidelsturz^{171,mm} D. Reikher¹⁵¹ A. Rejz¹⁴¹ C. Rembser³⁶ A. Renardi⁴⁸ M. Renda^{27b}
M. B. Rendel¹¹⁰ F. Renner⁴⁸ A. G. Rennie¹⁶⁰ A. L. Rescia⁴⁸ S. Resconi^{71a} M. Ressegotti^{57b,57a} S. Rettie³⁶
J. G. Reyes Rivera¹⁰⁷ B. Reynolds¹¹⁹ E. Reynolds^{17a} O. L. Rezanova³⁷ P. Reznicek¹³³ N. Ribaric⁹¹
E. Ricci^{78a,78b} R. Richter¹¹⁰ S. Richter^{47a,47b} E. Richter-Was^{86b} M. Ridel¹²⁷ S. Ridouani^{35d} P. Rieck¹¹⁷
P. Riedler³⁶ M. Rijssenbeek¹⁴⁵ A. Rimoldi^{73a,73b} M. Rimoldi⁴⁸ L. Rinaldi^{23b,23a} T. T. Rinn²⁹
M. P. Rinnagel¹⁰⁹ G. Ripellino¹⁶¹ I. Riu¹³ P. Rivadeneira⁴⁸ J. C. Rivera Vergara¹⁶⁵ F. Rizatdinova¹²¹
E. Rizvi⁹⁴ B. A. Roberts¹⁶⁷ B. R. Roberts^{17a} S. H. Robertson^{104,q} D. Robinson³² C. M. Robles Gajardo^{137f}
M. Robles Manzano¹⁰⁰ A. Robson⁵⁹ A. Rocchi^{76a,76b} C. Roda^{74a,74b} S. Rodriguez Bosca^{63a}
Y. Rodriguez Garcia^{22a} A. Rodriguez Rodriguez⁵⁴ A. M. Rodriguez Vera^{156b} S. Roe³⁶ J. T. Roemer¹⁶⁰
A. R. Roepe-Gier¹³⁶ J. Roggel¹⁷¹ O. Røhne¹²⁵ R. A. Rojas¹⁰³ C. P. A. Roland⁶⁸ J. Roloff²⁹ A. Romaniouk³⁷
E. Romano^{73a,73b} M. Romano^{23b} A. C. Romero Hernandez¹⁶² N. Rompotis⁹² L. Roos¹²⁷ S. Rosati^{75a}
B. J. Rosser³⁹ E. Rossi¹²⁶ E. Rossi^{72a,72b} L. P. Rossi^{57b} L. Rossini⁵⁴ R. Rosten¹¹⁹ M. Rotaru^{27b}
B. Rottler⁵⁴ C. Rougier^{102,ii} D. Rousseau⁶⁶ D. Rousso³² A. Roy¹⁶² S. Roy-Garand¹⁵⁵ A. Rozanov¹⁰²
Y. Rozen¹⁵⁰ X. Ruan^{33g} A. Rubio Jimenez¹⁶³ A. J. Ruby⁹² V. H. Ruelas Rivera¹⁸ T. A. Ruggeri¹
A. Ruggiero¹²⁶ A. Ruiz-Martinez¹⁶³ A. Rummeler³⁶ Z. Rurikova⁵⁴ N. A. Rusakovich³⁸ H. L. Russell¹⁶⁵

G. Russo^{75a,75b} J. P. Rutherford⁷ S. Rutherford Colmenares³² K. Rybacki⁹¹ M. Rybar¹³³ E. B. Rye¹²⁵
A. Ryzhov⁴⁴ J. A. Sabater Iglesias⁵⁶ P. Sabatini¹⁶³ L. Sabetta^{75a,75b} H. F-W. Sadrozinski¹³⁶ F. Safai Tehrani^{75a}
B. Safarzadeh Samani¹⁴⁶ M. Safdari¹⁴³ S. Saha¹⁶⁵ M. Sahinsoy¹¹⁰ M. Saimpert¹³⁵ M. Saito¹⁵³ T. Saito¹⁵³
D. Salamani³⁶ A. Salnikov¹⁴³ J. Salt¹⁶³ A. Salvador Salas¹³ D. Salvatore^{43b,43a} F. Salvatore¹⁴⁶
A. Salzburger³⁶ D. Sammel⁵⁴ D. Sampsonidis^{152,cc} D. Sampsonidou¹²³ J. Sánchez¹⁶³ A. Sanchez Pineda⁴
V. Sanchez Sebastian¹⁶³ H. Sandaker¹²⁵ C. O. Sander⁴⁸ J. A. Sandesara¹⁰³ M. Sandhoff¹⁷¹ C. Sandoval^{22b}
D. P. C. Sankey¹³⁴ T. Sano⁸⁸ A. Sansoni⁵³ L. Santi^{75a,75b} C. Santoni⁴⁰ H. Santos^{130a,130b} S. N. Santpur^{17a}
A. Santra¹⁶⁹ K. A. Saoucha¹³⁹ J. G. Saraiva^{130a,130d} J. Sardain⁷ O. Sasaki⁸⁴ K. Sato¹⁵⁷ C. Sauer^{63b}
F. Sauerburger⁵⁴ E. Sauvan⁴ P. Savard^{155,e} R. Sawada¹⁵³ C. Sawyer¹³⁴ L. Sawyer⁹⁷ I. Sayago Galvan¹⁶³
C. Sbarra^{23b} A. Sbrizzi^{23b,23a} T. Scanlon⁹⁶ J. Schaarschmidt¹³⁸ P. Schacht¹¹⁰ D. Schaefer³⁹ U. Schäfer¹⁰⁰
A. C. Schaffer^{66,44} D. Schaile¹⁰⁹ R. D. Schamberger¹⁴⁵ C. Scharf¹⁸ M. M. Schefer¹⁹ V. A. Schegelsky³⁷
D. Scheirich¹³³ F. Schenck¹⁸ M. Schernau¹⁶⁰ C. Scheulen⁵⁵ C. Schiavi^{57b,57a} E. J. Schioppa^{70a,70b}
M. Schioppa^{43b,43a} B. Schlag^{143,u} K. E. Schleicher⁵⁴ S. Schlenker³⁶ J. Schmeing¹⁷¹ M. A. Schmidt¹⁷¹
K. Schmieden¹⁰⁰ C. Schmitt¹⁰⁰ S. Schmitt⁴⁸ L. Schoeffel¹³⁵ A. Schoening^{63b} P. G. Scholer⁵⁴ E. Schopf¹²⁶
M. Schott¹⁰⁰ J. Schovancova³⁶ S. Schramm⁵⁶ F. Schroeder¹⁷¹ T. Schroer⁵⁶ H-C. Schultz-Coulon^{63a}
M. Schumacher⁵⁴ B. A. Schumm¹³⁶ Ph. Schune¹³⁵ A. J. Schuy¹³⁸ H. R. Schwartz¹³⁶ A. Schwartzman¹⁴³
T. A. Schwarz¹⁰⁶ Ph. Schwemling¹³⁵ R. Schwienhorst¹⁰⁷ A. Sciandra¹³⁶ G. Sciolla²⁶ F. Scuri^{74a}
C. D. Sebastiani⁹² K. Sedlaczek¹¹⁵ P. Seema¹⁸ S. C. Seidel¹¹² A. Seiden¹³⁶ B. D. Seidlitz⁴¹ C. Seitz⁴⁸
J. M. Seixas^{83b} G. Sekhniaidze^{72a} S. J. Sekula⁴⁴ L. Selem⁶⁰ N. Semprini-Cesari^{23b,23a} D. Sengupta⁵⁶
V. Senthilkumar¹⁶³ L. Serin⁶⁶ L. Serkin^{69a,69b} M. Sessa^{76a,76b} H. Severini¹²⁰ F. Sforza^{57b,57a} A. Sfyrla⁵⁶
E. Shabalina⁵⁵ R. Shaheen¹⁴⁴ J. D. Shahinian¹²⁸ D. Shaked Renous¹⁶⁹ L. Y. Shan^{14a} M. Shapiro^{17a}
A. Sharma³⁶ A. S. Sharma¹⁶⁴ P. Sharma⁸⁰ S. Sharma⁴⁸ P. B. Shatalov³⁷ K. Shaw¹⁴⁶ S. M. Shaw¹⁰¹
A. Shcherbakova³⁷ Q. Shen^{62c,5} P. Sherwood⁹⁶ L. Shi⁹⁶ X. Shi^{14a} C. O. Shimmin¹⁷² Y. Shimogama¹⁶⁸
J. D. Shinner⁹⁵ I. P. J. Shipsey¹²⁶ S. Shirabe^{56,kk} M. Shiyakova^{38,nn} J. Shlomi¹⁶⁹ M. J. Shochet³⁹ J. Shojaii¹⁰⁵
D. R. Shope¹²⁵ B. Shrestha¹²⁰ S. Shrestha^{119,oo} E. M. Shrif^{33g} M. J. Shroff¹⁶⁵ P. Sicho¹³¹ A. M. Sickles¹⁶²
E. Sideras Haddad^{33g} A. Sidoti^{23b} F. Siegert⁵⁰ Dj. Sijacki¹⁵ R. Sikora^{86a} F. Sili⁹⁰ J. M. Silva²⁰
M. V. Silva Oliveira²⁹ S. B. Silverstein^{47a} S. Simion⁶⁶ R. Simoniello³⁶ E. L. Simpson⁵⁹ H. Simpson¹⁴⁶
L. R. Simpson¹⁰⁶ N. D. Simpson⁹⁸ S. Simsek⁸² S. Sindhu⁵⁵ P. Sinervo¹⁵⁵ S. Singh¹⁵⁵ S. Sinha⁴⁸ S. Sinha¹⁰¹
M. Sioli^{23b,23a} I. Siral³⁶ E. Sitnikova⁴⁸ S. Yu. Sivoklovov^{37,a} J. Sjölin^{47a,47b} A. Skaf⁵⁵ E. Skorda^{20,pp}
P. Skubic¹²⁰ M. Slawinska⁸⁷ V. Smakhtin¹⁶⁹ B. H. Smart¹³⁴ J. Smiesko³⁶ S. Yu. Smirnov³⁷ Y. Smirnov³⁷
L. N. Smirnova^{37,m} O. Smirnova⁹⁸ A. C. Smith⁴¹ E. A. Smith³⁹ H. A. Smith¹²⁶ J. L. Smith⁹² R. Smith¹⁴³
M. Smizanska⁹¹ K. Smolek¹³² A. A. Snesarev³⁷ S. R. Snider¹⁵⁵ H. L. Snoek¹¹⁴ S. Snyder²⁹ R. Sobie^{165,q}
A. Soffer¹⁵¹ C. A. Solans Sanchez³⁶ E. Yu. Soldatov³⁷ U. Soldevila¹⁶³ A. A. Solodkov³⁷ S. Solomon²⁶
A. Soloshenko³⁸ K. Solovieva⁵⁴ O. V. Solovyanov⁴⁰ V. Solovyev³⁷ P. Sommer³⁶ A. Sonay¹³ W. Y. Song^{156b}
J. M. Sonneveld¹¹⁴ A. Sopczak¹³² A. L. Soppio⁹⁶ F. Sopkova^{28b} V. Sothilingam^{63a} S. Sottocornola⁶⁸
R. Soualah^{116b} Z. Soumami^{35e} D. South⁴⁸ N. Soybelman¹⁶⁹ S. Spagnolo^{70a,70b} M. Spalla¹¹⁰ D. Sperlich⁵⁴
G. Spigo³⁶ M. Spina¹⁴⁶ S. Spinali⁹¹ D. P. Spiteri⁵⁹ M. Spusta¹³³ E. J. Staats³⁴ A. Stabile^{71a,71b}
R. Stamen^{63a} A. Stampekis²⁰ M. Standke²⁴ E. Stanecka⁸⁷ M. V. Stange⁵⁰ B. Stanislaus^{17a} M. M. Stanitzki⁴⁸
B. Stapf⁴⁸ E. A. Starchenko³⁷ G. H. Stark¹³⁶ J. Stark^{102,ii} D. M. Starko^{156b} P. Staroba¹³¹ P. Starovoitov^{63a}
S. Stärz¹⁰⁴ R. Staszewski⁸⁷ G. Stavropoulos⁴⁶ J. Steentoft¹⁶¹ P. Steinberg²⁹ B. Stelzer^{142,156a} H. J. Stelzer¹²⁹
O. Stelzer-Chilton^{156a} H. Stenzel⁵⁸ T. J. Stevenson¹⁴⁶ G. A. Stewart³⁶ J. R. Stewart¹²¹ M. C. Stockton³⁶
G. Stoicea^{27b} M. Stolarski^{130a} S. Stonjek¹¹⁰ A. Straessner⁵⁰ J. Strandberg¹⁴⁴ S. Strandberg^{47a,47b}
M. Strauss¹²⁰ T. Strebler¹⁰² P. Strizenec^{28b} R. Ströhmer¹⁶⁶ D. M. Strom¹²³ L. R. Strom⁴⁸ R. Stroynowski⁴⁴
A. Strubig^{47a,47b} S. A. Stucci²⁹ B. Stugu¹⁶ J. Stupak¹²⁰ N. A. Styles⁴⁸ D. Su¹⁴³ S. Su^{62a} W. Su^{62d}
X. Su^{62a,66} K. Sugizaki¹⁵³ V. V. Sulim³⁷ M. J. Sullivan⁹² D. M. S. Sultan^{78a,78b} L. Sultanaliyeva³⁷
S. Sultansoy^{3b} T. Sumida⁸⁸ S. Sun¹⁰⁶ S. Sun¹⁷⁰ O. Sunneborn Gudnadottir¹⁶¹ N. Sur¹⁰² M. R. Sutton¹⁴⁶
H. Suzuki¹⁵⁷ M. Svatos¹³¹ M. Swiatlowski^{156a} T. Swirski¹⁶⁶ I. Sykora^{28a} M. Sykora¹³³ T. Sykora¹³³
D. Ta¹⁰⁰ K. Tackmann^{48,qq} A. Taffard¹⁶⁰ R. Tafirout^{156a} J. S. Tafuya Vargas⁶⁶ E. P. Takeva⁵² Y. Takubo⁸⁴
M. Talby¹⁰² A. A. Talyshv³⁷ K. C. Tam^{64b} N. M. Tamir¹⁵¹ A. Tanaka¹⁵³ J. Tanaka¹⁵³ R. Tanaka⁶⁶

M. Tanasini^{57b,57a} Z. Tao¹⁶⁴ S. Tapia Araya^{137f} S. Tapprogge¹⁰⁰ A. Tarek Abouelfadl Mohamed¹⁰⁷ S. Tarem¹⁵⁰
 K. Tariq^{14a} G. Tarna^{102,27b} G. F. Tartarelli^{71a} P. Tas¹³³ M. Tasevsky¹³¹ E. Tassi^{43b,43a} A. C. Tate¹⁶²
 G. Tateno¹⁵³ Y. Tayalati^{35e,rr} G. N. Taylor¹⁰⁵ W. Taylor^{156b} H. Teagle⁹² A. S. Tee¹⁷⁰ R. Teixeira De Lima¹⁴³
 P. Teixeira-Dias⁹⁵ J. J. Teoh¹⁵⁵ K. Terashi¹⁵³ J. Terron⁹⁹ S. Terzo¹³ M. Testa⁵³ R. J. Teuscher^{155,q}
 A. Thaler⁷⁹ O. Theiner⁵⁶ N. Themistokleous⁵² T. Theveneaux-Pelzer¹⁰² O. Thielmann¹⁷¹ D. W. Thomas⁹⁵
 J. P. Thomas²⁰ E. A. Thompson^{17a} P. D. Thompson²⁰ E. Thomson¹²⁸ Y. Tian⁵⁵ V. Tikhomirov^{37,m}
 Yu. A. Tikhonov³⁷ S. Timoshenko³⁷ D. Timoshyn¹³³ E. X. L. Ting¹ P. Tipton¹⁷² S. H. Tlou^{33g} A. Tnourji⁴⁰
 K. Todome^{23b,23a} S. Todorova-Nova¹³³ S. Todt⁵⁰ M. Togawa⁸⁴ J. Tojo⁸⁹ S. Tokár^{28a} K. Tokushuku⁸⁴
 O. Toldaiev⁶⁸ R. Tombs³² M. Tomoto^{84,111} L. Tompkins^{143,u} K. W. Topolnicki^{86b} E. Torrence¹²³
 H. Torres^{102,ii} E. Torró Pastor¹⁶³ M. Toscani³⁰ C. Toscirì³⁹ M. Tost¹¹ D. R. Tovey¹³⁹ A. Traet¹⁶
 I. S. Trandafir^{27b} T. Trefzger¹⁶⁶ A. Tricoli²⁹ I. M. Trigger^{156a} S. Trincaz-Duvoid¹²⁷ D. A. Trischuk²⁶
 B. Trocme⁶⁰ C. Troncon^{71a} L. Truong^{33c} M. Trzebinski⁸⁷ A. Trzuppek⁸⁷ F. Tsai¹⁴⁵ M. Tsai¹⁰⁶
 A. Tsiamis^{152,cc} P. V. Tsiarehka³⁷ S. Tsigaridas^{156a} A. Tsirigotis^{152,dd} V. Tsiskaridze¹⁵⁵ E. G. Tskhadadze^{149a}
 M. Tsopoulou^{152,cc} Y. Tsujikawa⁸⁸ I. I. Tsukerman³⁷ V. Tsulaia^{17a} S. Tsuno⁸⁴ O. Tsur¹⁵⁰ K. Tsurii¹¹⁸
 D. Tsybychev¹⁴⁵ Y. Tu^{64b} A. Tudorache^{27b} V. Tudorache^{27b} A. N. Tuna³⁶ S. Turchikhin³⁸ I. Turk Cakir^{3a}
 R. Turra^{71a} T. Turtuvshin^{38,ss} P. M. Tuts⁴¹ S. Tzamaris^{152,cc} P. Tzanis¹⁰ E. Tzovara¹⁰⁰ K. Uchida¹⁵³
 F. Ukegawa¹⁵⁷ P. A. Ulloa Poblete^{137c,137b} E. N. Umaka²⁹ G. Unal³⁶ M. Unal¹¹ A. Undrus²⁹ G. Unel¹⁶⁰
 J. Urban^{28b} P. Urquijo¹⁰⁵ G. Usai⁸ R. Ushioda¹⁵⁴ M. Usman¹⁰⁸ Z. Uysal^{21b} L. Vacavant¹⁰² V. Vacek¹³²
 B. Vachon¹⁰⁴ K. O. H. Vadla¹²⁵ T. Vafeiadis³⁶ A. Vaitkus⁹⁶ C. Valderanis¹⁰⁹ E. Valdes Santurio^{47a,47b}
 M. Valente^{156a} S. Valentinetti^{23b,23a} A. Valero¹⁶³ E. Valiente Moreno¹⁶³ A. Vallier^{102,ii} J. A. Valls Ferrer¹⁶³
 D. R. Van Arneman¹¹⁴ T. R. Van Daalen¹³⁸ A. Van Der Graaf⁴⁹ P. Van Gemmeren⁶ M. Van Rijnbach^{125,36}
 S. Van Stroud⁹⁶ I. Van Vulpen¹¹⁴ M. Vanadia^{76a,76b} W. Vandelli³⁶ M. Vandenbroucke¹³⁵ E. R. Vandewall¹²¹
 D. Vannicola¹⁵¹ L. Vannoli^{57b,57a} R. Vari^{75a} E. W. Varnes⁷ C. Varni^{17b} T. Varol¹⁴⁸ D. Varouchas⁶⁶
 L. Varriale¹⁶³ K. E. Varvell¹⁴⁷ M. E. Vasile^{27b} L. Vaslin⁴⁰ G. A. Vasquez¹⁶⁵ A. Vasyukov³⁸ F. Vazeille⁴⁰
 T. Vazquez Schroeder³⁶ J. Veatch³¹ V. Vecchio¹⁰¹ M. J. Veen¹⁰³ I. Veliscek¹²⁶ L. M. Veloce¹⁵⁵
 F. Veloso^{130a,130c} S. Veneziano^{75a} A. Ventura^{70a,70b} A. Verbytskyi¹¹⁰ M. Verducci^{74a,74b} C. Vergis²⁴
 M. Verissimo De Araujo^{83b} W. Verkerke¹¹⁴ J. C. Vermeulen¹¹⁴ C. Vernieri¹⁴³ M. Vessella¹⁰³ M. C. Vetterli^{142,e}
 A. Vgenopoulos^{152,cc} N. Viaux Maira^{137f} T. Vickey¹³⁹ O. E. Vickey Boeriu¹³⁹ G. H. A. Viehhauser¹²⁶
 L. Vigani^{63b} M. Villa^{23b,23a} M. Villaplana Perez¹⁶³ E. M. Villhauer⁵² E. Vilucchi⁵³ M. G. Vincter³⁴
 G. S. Virdee²⁰ A. Vishwakarma⁵² A. Visibile¹¹⁴ C. Vittori³⁶ I. Vivarelli¹⁴⁶ V. Vladimirov¹⁶⁷ E. Voevodina¹¹⁰
 F. Vogel¹⁰⁹ P. Vokac¹³² J. Von Ahnen⁴⁸ E. Von Toerne²⁴ B. Vormwald³⁶ V. Vorobel¹³³ K. Vorobev³⁷
 M. Vos¹⁶³ K. Voss¹⁴¹ J. H. Vossebeld⁹² M. Vozak¹¹⁴ L. Vozdecky⁹⁴ N. Vranjes¹⁵
 M. Vranjes Milosavljevic¹⁵ M. Vreeswijk¹¹⁴ N. K. Vu^{62d,62c} R. Vuillermet³⁶ O. Vujanovic¹⁰⁰ I. Vukotic³⁹
 S. Wada¹⁵⁷ C. Wagner¹⁰³ J. M. Wagner^{17a} W. Wagner¹⁷¹ S. Wahdan¹⁷¹ H. Wahlberg⁹⁰ R. Wakasa¹⁵⁷
 M. Wakida¹¹¹ J. Walder¹³⁴ R. Walker¹⁰⁹ W. Walkowiak¹⁴¹ A. Wall¹²⁸ T. Wamorkar⁶ A. Z. Wang¹⁷⁰
 C. Wang¹⁰⁰ C. Wang^{62c} H. Wang^{17a} J. Wang^{64a} R.-J. Wang¹⁰⁰ R. Wang⁶¹ R. Wang⁶ S. M. Wang¹⁴⁸
 S. Wang^{62b} T. Wang^{62a} W. T. Wang⁸⁰ W. Wang^{14a} X. Wang^{14c} X. Wang¹⁶² X. Wang^{62c} Y. Wang^{62d}
 Y. Wang^{14c} Z. Wang¹⁰⁶ Z. Wang^{62d,51,62c} Z. Wang¹⁰⁶ A. Warburton¹⁰⁴ R. J. Ward²⁰ N. Warrack⁵⁹
 A. T. Watson²⁰ H. Watson⁵⁹ M. F. Watson²⁰ E. Watton^{59,134} G. Watts¹³⁸ B. M. Waugh⁹⁶ C. Weber²⁹
 H. A. Weber¹⁸ M. S. Weber¹⁹ S. M. Weber^{63a} C. Wei^{62a} Y. Wei¹²⁶ A. R. Weidberg¹²⁶ E. J. Weik¹¹⁷
 J. Weingarten⁴⁹ M. Weirich¹⁰⁰ C. Weiser⁵⁴ C. J. Wells⁴⁸ T. Wenaus²⁹ B. Wendland⁴⁹ T. Wengler³⁶
 N. S. Wenke¹¹⁰ N. Wermes²⁴ M. Wessels^{63a} K. Whalen¹²³ A. M. Wharton⁹¹ A. S. White⁶¹ A. White⁸
 M. J. White¹ D. Whiteson¹⁶⁰ L. Wickremasinghe¹²⁴ W. Wiedenmann¹⁷⁰ C. Wiel⁵⁰ M. Wielers¹³⁴
 C. Wiglesworth⁴² D. J. Wilbern¹²⁰ H. G. Wilkens³⁶ D. M. Williams⁴¹ H. H. Williams¹²⁸ S. Williams³²
 S. Willocq¹⁰³ B. J. Wilson¹⁰¹ P. J. Windischhofer³⁹ F. I. Winkel³⁰ F. Winklmeier¹²³ B. T. Winter⁵⁴
 J. K. Winter¹⁰¹ M. Wittgen¹⁴³ M. Wobisch⁹⁷ Z. Wolffs¹¹⁴ R. Wölker¹²⁶ J. Wollrath¹⁶⁰ M. W. Wolter⁸⁷
 H. Wolters^{130a,130c} A. F. Wongel⁴⁸ S. D. Worm⁴⁸ B. K. Wosiek⁸⁷ K. W. Woźniak⁸⁷ S. Wozniowski⁵⁵
 K. Wraight⁵⁹ C. Wu²⁰ J. Wu^{14a,14e} M. Wu^{64a} M. Wu¹¹³ S. L. Wu¹⁷⁰ X. Wu⁵⁶ Y. Wu^{62a} Z. Wu¹³⁵
 J. Wuerzinger^{110,x} T. R. Wyatt¹⁰¹ B. M. Wynne⁵² S. Xella⁴² L. Xia^{14c} M. Xia^{14b} J. Xiang^{64c} X. Xiao¹⁰⁶

M. Xie^{62a}, X. Xie^{62a}, S. Xin^{14a,14e}, J. Xiong^{17a}, D. Xu^{14a}, H. Xu^{62a}, L. Xu^{62a}, R. Xu¹²⁸, T. Xu¹⁰⁶, Y. Xu^{14b},
 Z. Xu⁵², Z. Xu^{14a}, B. Yabsley¹⁴⁷, S. Yacoob^{33a}, N. Yamaguchi⁸⁹, Y. Yamaguchi¹⁵⁴, E. Yamashita¹⁵³,
 H. Yamauchi¹⁵⁷, T. Yamazaki^{17a}, Y. Yamazaki⁸⁵, J. Yan^{62c}, S. Yan¹²⁶, Z. Yan²⁵, H. J. Yang^{62c,62d}, H. T. Yang^{62a},
 S. Yang^{62a}, T. Yang^{64c}, X. Yang^{62a}, X. Yang^{14a}, Y. Yang⁴⁴, Y. Yang^{62a}, Z. Yang^{62a}, W-M. Yao^{17a}, Y. C. Yap⁴⁸,
 H. Ye^{14c}, H. Ye⁵⁵, J. Ye⁴⁴, S. Ye²⁹, X. Ye^{62a}, Y. Yeh⁹⁶, I. Yeletsikh³⁸, B. K. Yeo^{17b}, M. R. Yexley⁹⁶,
 P. Yin⁴¹, K. Yorita¹⁶⁸, S. Younas^{27b}, C. J. S. Young³⁶, C. Young¹⁴³, Y. Yu^{62a}, M. Yuan¹⁰⁶, R. Yuan^{62b,tt},
 L. Yue⁹⁶, M. Zaazoua^{62a}, B. Zabinski⁸⁷, E. Zaid⁵², T. Zakareishvili^{149b}, N. Zakharchuk³⁴, S. Zambito⁵⁶,
 J. A. Zamora Saa^{137d,137b}, J. Zang¹⁵³, D. Zanzi⁵⁴, O. Zaplatilek¹³², C. Zeitnitz¹⁷¹, H. Zeng^{14a}, J. C. Zeng¹⁶²,
 D. T. Zenger Jr.²⁶, O. Zenin³⁷, T. Ženiš^{28a}, S. Zenz⁹⁴, S. Zerradi^{35a}, D. Zerwas⁶⁶, M. Zhai^{14a,14e}, B. Zhang^{14c},
 D. F. Zhang¹³⁹, J. Zhang^{62b}, J. Zhang⁶, K. Zhang^{14a,14e}, L. Zhang^{14c}, P. Zhang^{14a,14e}, R. Zhang¹⁷⁰, S. Zhang¹⁰⁶,
 T. Zhang¹⁵³, X. Zhang^{62c}, X. Zhang^{62b}, Y. Zhang^{62c,5}, Y. Zhang⁹⁶, Z. Zhang^{17a}, Z. Zhang⁶⁶, H. Zhao¹³⁸,
 P. Zhao⁵¹, T. Zhao^{62b}, Y. Zhao¹³⁶, Z. Zhao^{62a}, A. Zhemchugov³⁸, J. Zheng^{14c}, K. Zheng¹⁶², X. Zheng^{62a},
 Z. Zheng¹⁴³, D. Zhong¹⁶², B. Zhou¹⁰⁶, H. Zhou⁷, N. Zhou^{62c}, Y. Zhou⁷, C. G. Zhu^{62b}, J. Zhu¹⁰⁶, Y. Zhu^{62c},
 Y. Zhu^{62a}, X. Zhuang^{14a}, K. Zhukov³⁷, V. Zhulanov³⁷, N. I. Zimine³⁸, J. Zinsser^{63b}, M. Ziolkowski¹⁴¹,
 L. Živković¹⁵, A. Zoccoli^{23b,23a}, K. Zoch⁵⁶, T. G. Zorbass¹³⁹, O. Zormpa⁴⁶, W. Zou⁴¹ and L. Zwalinski³⁶

(ATLAS Collaboration)

¹*Department of Physics, University of Adelaide, Adelaide, Australia*

²*Department of Physics, University of Alberta, Edmonton, Alberta, Canada*

^{3a}*Department of Physics, Ankara University, Ankara, Türkiye*

^{3b}*Division of Physics, TOBB University of Economics and Technology, Ankara, Türkiye*

⁴*LAPP, Université Savoie Mont Blanc, CNRS/IN2P3, Annecy, France*

⁵*APC, Université Paris Cité, CNRS/IN2P3, Paris, France*

⁶*High Energy Physics Division, Argonne National Laboratory, Argonne, Illinois, USA*

⁷*Department of Physics, University of Arizona, Tucson, Arizona, USA*

⁸*Department of Physics, University of Texas at Arlington, Arlington, Texas, USA*

⁹*Physics Department, National and Kapodistrian University of Athens, Athens, Greece*

¹⁰*Physics Department, National Technical University of Athens, Zografou, Greece*

¹¹*Department of Physics, University of Texas at Austin, Austin, Texas, USA*

¹²*Institute of Physics, Azerbaijan Academy of Sciences, Baku, Azerbaijan*

¹³*Institut de Física d'Altes Energies (IFAE), Barcelona Institute of Science and Technology, Barcelona, Spain*

^{14a}*Institute of High Energy Physics, Chinese Academy of Sciences, Beijing, China*

^{14b}*Physics Department, Tsinghua University, Beijing, China*

^{14c}*Department of Physics, Nanjing University, Nanjing, China*

^{14d}*School of Science, Shenzhen Campus of Sun Yat-sen University, China*

^{14e}*University of Chinese Academy of Science (UCAS), Beijing, China*

¹⁵*Institute of Physics, University of Belgrade, Belgrade, Serbia*

¹⁶*Department for Physics and Technology, University of Bergen, Bergen, Norway*

^{17a}*Physics Division, Lawrence Berkeley National Laboratory, Berkeley, California, USA*

^{17b}*University of California, Berkeley, California, USA*

¹⁸*Institut für Physik, Humboldt Universität zu Berlin, Berlin, Germany*

¹⁹*Albert Einstein Center for Fundamental Physics and Laboratory for High Energy Physics, University of Bern, Bern, Switzerland*

²⁰*School of Physics and Astronomy, University of Birmingham, Birmingham, United Kingdom*

^{21a}*Department of Physics, Bogazici University, Istanbul, Türkiye*

^{21b}*Department of Physics Engineering, Gaziantep University, Gaziantep, Türkiye*

^{21c}*Department of Physics, Istanbul University, Istanbul, Türkiye*

^{22a}*Facultad de Ciencias y Centro de Investigaciones, Universidad Antonio Nariño, Bogotá, Colombia*

^{22b}*Departamento de Física, Universidad Nacional de Colombia, Bogotá, Colombia*

^{23a}*Dipartimento di Fisica e Astronomia A. Righi, Università di Bologna, Bologna, Italy*

^{23b}*INFN Sezione di Bologna, Bologna, Italy*

²⁴*Physikalisches Institut, Universität Bonn, Bonn, Germany*

²⁵*Department of Physics, Boston University, Boston, Massachusetts, USA*

²⁶*Department of Physics, Brandeis University, Waltham, Massachusetts, USA*

- ^{27a}Transilvania University of Brasov, Brasov, Romania
- ^{27b}Horia Hulubei National Institute of Physics and Nuclear Engineering, Bucharest, Romania
- ^{27c}Department of Physics, Alexandru Ioan Cuza University of Iasi, Iasi, Romania
- ^{27d}National Institute for Research and Development of Isotopic and Molecular Technologies, Physics Department, Cluj-Napoca, Romania
- ^{27e}University Politehnica Bucharest, Bucharest, Romania
- ^{27f}West University in Timisoara, Timisoara, Romania
- ^{27g}Faculty of Physics, University of Bucharest, Bucharest, Romania
- ^{28a}Faculty of Mathematics, Physics and Informatics, Comenius University, Bratislava, Slovak Republic
- ^{28b}Department of Subnuclear Physics, Institute of Experimental Physics of the Slovak Academy of Sciences, Kosice, Slovak Republic
- ²⁹Physics Department, Brookhaven National Laboratory, Upton, New York, USA
- ³⁰Universidad de Buenos Aires, Facultad de Ciencias Exactas y Naturales, Departamento de Física, y CONICET, Instituto de Física de Buenos Aires (IFIBA), Buenos Aires, Argentina
- ³¹California State University, Hayward, California, USA
- ³²Cavendish Laboratory, University of Cambridge, Cambridge, United Kingdom
- ^{33a}Department of Physics, University of Cape Town, Cape Town, South Africa
- ^{33b}iThemba Labs, Western Cape, South Africa
- ^{33c}Department of Mechanical Engineering Science, University of Johannesburg, Johannesburg, South Africa
- ^{33d}National Institute of Physics, University of the Philippines Diliman (Philippines), Quezon City, Philippines
- ^{33e}University of South Africa, Department of Physics, Pretoria, South Africa
- ^{33f}University of Zululand, KwaDlangezwa, South Africa
- ^{33g}School of Physics, University of the Witwatersrand, Johannesburg, South Africa
- ³⁴Department of Physics, Carleton University, Ottawa, Ontario, Canada
- ^{35a}Faculté des Sciences Ain Chock, Réseau Universitaire de Physique des Hautes Energies—Université Hassan II, Casablanca, Morocco
- ^{35b}Faculté des Sciences, Université Ibn-Tofail, Kénitra, Morocco
- ^{35c}Faculté des Sciences Semlalia, Université Cadi Ayyad, LPHEA-Marrakech, Morocco
- ^{35d}LPMR, Faculté des Sciences, Université Mohamed Premier, Oujda, Morocco
- ^{35e}Faculté des sciences, Université Mohammed V, Rabat, Morocco
- ^{35f}Institute of Applied Physics, Mohammed VI Polytechnic University, Ben Guerir, Morocco
- ³⁶CERN, Geneva, Switzerland
- ³⁷Affiliated with an institute covered by a cooperation agreement with CERN
- ³⁸Affiliated with an international laboratory covered by a cooperation agreement with CERN
- ³⁹Enrico Fermi Institute, University of Chicago, Chicago, Illinois, USA
- ⁴⁰LPC, Université Clermont Auvergne, CNRS/IN2P3, Clermont-Ferrand, France
- ⁴¹Nevis Laboratory, Columbia University, Irvington, New York, USA
- ⁴²Niels Bohr Institute, University of Copenhagen, Copenhagen, Denmark
- ^{43a}Dipartimento di Fisica, Università della Calabria, Rende, Italy
- ^{43b}INFN Gruppo Collegato di Cosenza, Laboratori Nazionali di Frascati, Italy
- ⁴⁴Physics Department, Southern Methodist University, Dallas, Texas, USA
- ⁴⁵Physics Department, University of Texas at Dallas, Richardson, Texas, USA
- ⁴⁶National Centre for Scientific Research “Demokritos,” Agia Paraskevi, Greece
- ^{47a}Department of Physics, Stockholm University, Stockholm, Sweden
- ^{47b}Oskar Klein Centre, Stockholm, Sweden
- ⁴⁸Deutsches Elektronen-Synchrotron DESY, Hamburg and Zeuthen, Germany
- ⁴⁹Fakultät Physik, Technische Universität Dortmund, Dortmund, Germany
- ⁵⁰Institut für Kern- und Teilchenphysik, Technische Universität Dresden, Dresden, Germany
- ⁵¹Department of Physics, Duke University, Durham, North Carolina, USA
- ⁵²SUPA—School of Physics and Astronomy, University of Edinburgh, Edinburgh, United Kingdom
- ⁵³INFN e Laboratori Nazionali di Frascati, Frascati, Italy
- ⁵⁴Physikalisches Institut, Albert-Ludwigs-Universität Freiburg, Freiburg, Germany
- ⁵⁵II. Physikalisches Institut, Georg-August-Universität Göttingen, Göttingen, Germany
- ⁵⁶Département de Physique Nucléaire et Corpusculaire, Université de Genève, Genève, Switzerland
- ^{57a}Dipartimento di Fisica, Università di Genova, Genova, Italy
- ^{57b}INFN Sezione di Genova, Genova, Italy
- ⁵⁸II. Physikalisches Institut, Justus-Liebig-Universität Giessen, Giessen, Germany
- ⁵⁹SUPA—School of Physics and Astronomy, University of Glasgow, Glasgow, United Kingdom

- ⁶⁰*LPSC, Université Grenoble Alpes, CNRS/IN2P3, Grenoble INP, Grenoble, France*
- ⁶¹*Laboratory for Particle Physics and Cosmology, Harvard University, Cambridge, Massachusetts, USA*
- ^{62a}*Department of Modern Physics and State Key Laboratory of Particle Detection and Electronics, University of Science and Technology of China, Hefei, China*
- ^{62b}*Institute of Frontier and Interdisciplinary Science and Key Laboratory of Particle Physics and Particle Irradiation (MOE), Shandong University, Qingdao, China*
- ^{62c}*School of Physics and Astronomy, Shanghai Jiao Tong University, Key Laboratory for Particle Astrophysics and Cosmology (MOE), SKLPPC, Shanghai, China*
- ^{62d}*Tsung-Dao Lee Institute, Shanghai, China*
- ^{63a}*Kirchhoff-Institut für Physik, Ruprecht-Karls-Universität Heidelberg, Heidelberg, Germany*
- ^{63b}*Physikalisches Institut, Ruprecht-Karls-Universität Heidelberg, Heidelberg, Germany*
- ^{64a}*Department of Physics, Chinese University of Hong Kong, Shatin, New Territories, Hong Kong, China*
- ^{64b}*Department of Physics, University of Hong Kong, Hong Kong, China*
- ^{64c}*Department of Physics and Institute for Advanced Study, Hong Kong University of Science and Technology, Clear Water Bay, Kowloon, Hong Kong, China*
- ⁶⁵*Department of Physics, National Tsing Hua University, Hsinchu, Taiwan*
- ⁶⁶*IJCLab, Université Paris-Saclay, CNRS/IN2P3, 91405, Orsay, France*
- ⁶⁷*Centro Nacional de Microelectrónica (IMB-CNM-CSIC), Barcelona, Spain*
- ⁶⁸*Department of Physics, Indiana University, Bloomington, Indiana, USA*
- ^{69a}*INFN Gruppo Collegato di Udine, Sezione di Trieste, Udine, Italy*
- ^{69b}*ICTP, Trieste, Italy*
- ^{69c}*Dipartimento Politecnico di Ingegneria e Architettura, Università di Udine, Udine, Italy*
- ^{70a}*INFN Sezione di Lecce, Lecce, Italy*
- ^{70b}*Dipartimento di Matematica e Fisica, Università del Salento, Lecce, Italy*
- ^{71a}*INFN Sezione di Milano, Milan, Italy*
- ^{71b}*Dipartimento di Fisica, Università di Milano, Milano, Italy*
- ^{72a}*INFN Sezione di Napoli, Naples, Italy*
- ^{72b}*Dipartimento di Fisica, Università di Napoli, Napoli, Italy*
- ^{73a}*INFN Sezione di Pavia, Pavia, Italy*
- ^{73b}*Dipartimento di Fisica, Università di Pavia, Pavia, Italy*
- ^{74a}*INFN Sezione di Pisa, Pisa, Italy*
- ^{74b}*Dipartimento di Fisica E. Fermi, Università di Pisa, Pisa, Italy*
- ^{75a}*INFN Sezione di Roma, Rome, Italy*
- ^{75b}*Dipartimento di Fisica, Sapienza Università di Roma, Roma, Italy*
- ^{76a}*INFN Sezione di Roma Tor Vergata, Rome, Italy*
- ^{76b}*Dipartimento di Fisica, Università di Roma Tor Vergata, Roma, Italy*
- ^{77a}*INFN Sezione di Roma Tre, Rome, Italy*
- ^{77b}*Dipartimento di Matematica e Fisica, Università Roma Tre, Roma, Italy*
- ^{78a}*INFN-TIFPA, Trento, Italy*
- ^{78b}*Università degli Studi di Trento, Trento, Italy*
- ⁷⁹*Universität Innsbruck, Department of Astro and Particle Physics, Innsbruck, Austria*
- ⁸⁰*University of Iowa, Iowa City, Iowa, USA*
- ⁸¹*Department of Physics and Astronomy, Iowa State University, Ames, Iowa, USA*
- ⁸²*Istinye University, Sariyer, Istanbul, Türkiye*
- ^{83a}*Departamento de Engenharia Elétrica, Universidade Federal de Juiz de Fora (UFJF), Juiz de Fora, Brazil*
- ^{83b}*Universidade Federal do Rio De Janeiro COPPE/EE/IF, Rio de Janeiro, Brazil*
- ^{83c}*Instituto de Física, Universidade de São Paulo, São Paulo, Brazil*
- ^{83d}*Rio de Janeiro State University, Rio de Janeiro, Brazil*
- ⁸⁴*KEK, High Energy Accelerator Research Organization, Tsukuba, Japan*
- ⁸⁵*Graduate School of Science, Kobe University, Kobe, Japan*
- ^{86a}*AGH University of Krakow, Faculty of Physics and Applied Computer Science, Krakow, Poland*
- ^{86b}*Marian Smoluchowski Institute of Physics, Jagiellonian University, Krakow, Poland*
- ⁸⁷*Institute of Nuclear Physics Polish Academy of Sciences, Krakow, Poland*
- ⁸⁸*Faculty of Science, Kyoto University, Kyoto, Japan*
- ⁸⁹*Research Center for Advanced Particle Physics and Department of Physics, Kyushu University, Fukuoka, Japan*
- ⁹⁰*Instituto de Física La Plata, Universidad Nacional de La Plata and CONICET, La Plata, Argentina*
- ⁹¹*Physics Department, Lancaster University, Lancaster, United Kingdom*

- ⁹²*Oliver Lodge Laboratory, University of Liverpool, Liverpool, United Kingdom*
- ⁹³*Department of Experimental Particle Physics, Jožef Stefan Institute and Department of Physics, University of Ljubljana, Ljubljana, Slovenia*
- ⁹⁴*School of Physics and Astronomy, Queen Mary University of London, London, United Kingdom*
- ⁹⁵*Department of Physics, Royal Holloway University of London, Egham, United Kingdom*
- ⁹⁶*Department of Physics and Astronomy, University College London, London, United Kingdom*
- ⁹⁷*Louisiana Tech University, Ruston, Louisiana, USA*
- ⁹⁸*Fysiska institutionen, Lunds universitet, Lund, Sweden*
- ⁹⁹*Departamento de Física Teórica C-15 and CIAFF, Universidad Autónoma de Madrid, Madrid, Spain*
- ¹⁰⁰*Institut für Physik, Universität Mainz, Mainz, Germany*
- ¹⁰¹*School of Physics and Astronomy, University of Manchester, Manchester, United Kingdom*
- ¹⁰²*CPPM, Aix-Marseille Université, CNRS/IN2P3, Marseille, France*
- ¹⁰³*Department of Physics, University of Massachusetts, Amherst, Massachusetts, USA*
- ¹⁰⁴*Department of Physics, McGill University, Montreal, Quebec, Canada*
- ¹⁰⁵*School of Physics, University of Melbourne, Victoria, Australia*
- ¹⁰⁶*Department of Physics, University of Michigan, Ann Arbor, Michigan, USA*
- ¹⁰⁷*Department of Physics and Astronomy, Michigan State University, East Lansing, Michigan, USA*
- ¹⁰⁸*Group of Particle Physics, University of Montreal, Montreal, Quebec, Canada*
- ¹⁰⁹*Fakultät für Physik, Ludwig-Maximilians-Universität München, München, Germany*
- ¹¹⁰*Max-Planck-Institut für Physik (Werner-Heisenberg-Institut), München, Germany*
- ¹¹¹*Graduate School of Science and Kobayashi-Maskawa Institute, Nagoya University, Nagoya, Japan*
- ¹¹²*Department of Physics and Astronomy, University of New Mexico, Albuquerque, New Mexico, USA*
- ¹¹³*Institute for Mathematics, Astrophysics and Particle Physics, Radboud University/Nikhef, Nijmegen, Netherlands*
- ¹¹⁴*Nikhef National Institute for Subatomic Physics and University of Amsterdam, Amsterdam, Netherlands*
- ¹¹⁵*Department of Physics, Northern Illinois University, DeKalb, Illinois, USA*
- ^{116a}*New York University Abu Dhabi, Abu Dhabi, United Arab Emirates*
- ^{116b}*University of Sharjah, Sharjah, United Arab Emirates*
- ¹¹⁷*Department of Physics, New York University, New York, New York, USA*
- ¹¹⁸*Ochanomizu University, Otsuka, Bunkyo-ku, Tokyo, Japan*
- ¹¹⁹*The Ohio State University, Columbus, Ohio, USA*
- ¹²⁰*Homer L. Dodge Department of Physics and Astronomy, University of Oklahoma, Norman, Oklahoma, USA*
- ¹²¹*Department of Physics, Oklahoma State University, Stillwater, Oklahoma, USA*
- ¹²²*Palacký University, Joint Laboratory of Optics, Olomouc, Czech Republic*
- ¹²³*Institute for Fundamental Science, University of Oregon, Eugene, Oregon, USA*
- ¹²⁴*Graduate School of Science, Osaka University, Osaka, Japan*
- ¹²⁵*Department of Physics, University of Oslo, Oslo, Norway*
- ¹²⁶*Department of Physics, Oxford University, Oxford, United Kingdom*
- ¹²⁷*LPNHE, Sorbonne Université, Université Paris Cité, CNRS/IN2P3, Paris, France*
- ¹²⁸*Department of Physics, University of Pennsylvania, Philadelphia, Pennsylvania, USA*
- ¹²⁹*Department of Physics and Astronomy, University of Pittsburgh, Pittsburgh, Pennsylvania, USA*
- ^{130a}*Laboratório de Instrumentação e Física Experimental de Partículas—LIP, Lisboa, Portugal*
- ^{130b}*Departamento de Física, Faculdade de Ciências, Universidade de Lisboa, Lisboa, Portugal*
- ^{130c}*Departamento de Física, Universidade de Coimbra, Coimbra, Portugal*
- ^{130d}*Centro de Física Nuclear da Universidade de Lisboa, Lisboa, Portugal*
- ^{130e}*Departamento de Física, Universidade do Minho, Braga, Portugal*
- ^{130f}*Departamento de Física Teórica y del Cosmos, Universidad de Granada, Granada, Spain*
- ^{130g}*Departamento de Física, Instituto Superior Técnico, Universidade de Lisboa, Lisboa, Portugal*
- ¹³¹*Institute of Physics of the Czech Academy of Sciences, Prague, Czech Republic*
- ¹³²*Czech Technical University in Prague, Prague, Czech Republic*
- ¹³³*Charles University, Faculty of Mathematics and Physics, Prague, Czech Republic*
- ¹³⁴*Particle Physics Department, Rutherford Appleton Laboratory, Didcot, United Kingdom*
- ¹³⁵*IRFU, CEA, Université Paris-Saclay, Gif-sur-Yvette, France*
- ¹³⁶*Santa Cruz Institute for Particle Physics, University of California Santa Cruz, Santa Cruz, California, USA*
- ^{137a}*Departamento de Física, Pontificia Universidad Católica de Chile, Santiago, Chile*
- ^{137b}*Millennium Institute for Subatomic physics at high energy frontier (SAPHIR), Santiago, Chile*
- ^{137c}*Instituto de Investigación Multidisciplinario en Ciencia y Tecnología, y Departamento de Física, Universidad de La Serena, La Serena, Chile*

- ^{137d}*Universidad Andres Bello, Department of Physics, Santiago, Chile*
^{137e}*Instituto de Alta Investigación, Universidad de Tarapacá, Arica, Chile*
^{137f}*Departamento de Física, Universidad Técnica Federico Santa María, Valparaíso, Chile*
¹³⁸*Department of Physics, University of Washington, Seattle, Washington, USA*
¹³⁹*Department of Physics and Astronomy, University of Sheffield, Sheffield, United Kingdom*
¹⁴⁰*Department of Physics, Shinshu University, Nagano, Japan*
¹⁴¹*Department Physik, Universität Siegen, Siegen, Germany*
¹⁴²*Department of Physics, Simon Fraser University, Burnaby, British Columbia, Canada*
¹⁴³*SLAC National Accelerator Laboratory, Stanford, California, USA*
¹⁴⁴*Department of Physics, Royal Institute of Technology, Stockholm, Sweden*
¹⁴⁵*Departments of Physics and Astronomy, Stony Brook University, Stony Brook, New York, USA*
¹⁴⁶*Department of Physics and Astronomy, University of Sussex, Brighton, United Kingdom*
¹⁴⁷*School of Physics, University of Sydney, Sydney, Australia*
¹⁴⁸*Institute of Physics, Academia Sinica, Taipei, Taiwan*
^{149a}*E. Andronikashvili Institute of Physics, Iv. Javakhishvili Tbilisi State University, Tbilisi, Georgia*
^{149b}*High Energy Physics Institute, Tbilisi State University, Tbilisi, Georgia*
^{149c}*University of Georgia, Tbilisi, Georgia*
¹⁵⁰*Department of Physics, Technion, Israel Institute of Technology, Haifa, Israel*
¹⁵¹*Raymond and Beverly Sackler School of Physics and Astronomy, Tel Aviv University, Tel Aviv, Israel*
¹⁵²*Department of Physics, Aristotle University of Thessaloniki, Thessaloniki, Greece*
¹⁵³*International Center for Elementary Particle Physics and Department of Physics, University of Tokyo, Tokyo, Japan*
¹⁵⁴*Department of Physics, Tokyo Institute of Technology, Tokyo, Japan*
¹⁵⁵*Department of Physics, University of Toronto, Toronto, Ontario, Canada*
^{156a}*TRIUMF, Vancouver, British Columbia, Canada*
^{156b}*Department of Physics and Astronomy, York University, Toronto, Ontario, Canada*
¹⁵⁷*Division of Physics and Tomonaga Center for the History of the Universe, Faculty of Pure and Applied Sciences, University of Tsukuba, Tsukuba, Japan*
¹⁵⁸*Department of Physics and Astronomy, Tufts University, Medford, Massachusetts, USA*
¹⁵⁹*United Arab Emirates University, Al Ain, United Arab Emirates*
¹⁶⁰*Department of Physics and Astronomy, University of California Irvine, Irvine, California, USA*
¹⁶¹*Department of Physics and Astronomy, University of Uppsala, Uppsala, Sweden*
¹⁶²*Department of Physics, University of Illinois, Urbana, Illinois, USA*
¹⁶³*Instituto de Física Corpuscular (IFIC), Centro Mixto Universidad de Valencia—CSIC, Valencia, Spain*
¹⁶⁴*Department of Physics, University of British Columbia, Vancouver, British Columbia, Canada*
¹⁶⁵*Department of Physics and Astronomy, University of Victoria, Victoria, British Columbia, Canada*
¹⁶⁶*Fakultät für Physik und Astronomie, Julius-Maximilians-Universität Würzburg, Würzburg, Germany*
¹⁶⁷*Department of Physics, University of Warwick, Coventry, United Kingdom*
¹⁶⁸*Waseda University, Tokyo, Japan*
¹⁶⁹*Department of Particle Physics and Astrophysics, Weizmann Institute of Science, Rehovot, Israel*
¹⁷⁰*Department of Physics, University of Wisconsin, Madison, Wisconsin, USA*
¹⁷¹*Fakultät für Mathematik und Naturwissenschaften, Fachgruppe Physik, Bergische Universität Wuppertal, Wuppertal, Germany*
¹⁷²*Department of Physics, Yale University, New Haven, Connecticut, USA*

^aDeceased.

^bAlso at Department of Physics, King's College London, London, United Kingdom.

^cAlso at Institute of Physics, Azerbaijan Academy of Sciences, Baku, Azerbaijan.

^dAlso at Lawrence Livermore National Laboratory, Livermore, California, USA.

^eAlso at TRIUMF, Vancouver, British Columbia, Canada.

^fAlso at Department of Physics, University of Thessaly, Greece.

^gAlso at An-Najah National University, Nablus, Palestine.

^hAlso at Department of Physics, University of Fribourg, Fribourg, Switzerland.

ⁱAlso at University of Colorado Boulder, Department of Physics, Boulder, Colorado, USA.

^jAlso at Department of Physics and Astronomy, University of Victoria, Victoria, British Columbia, Canada.

^kAlso at Department of Physics, Westmont College, Santa Barbara, California, USA.

^lAlso at Departament de Física de la Universitat Autònoma de Barcelona, Barcelona, Spain.

^mAlso at Affiliated with an institute covered by a cooperation agreement with CERN.

ⁿAlso at The Collaborative Innovation Center of Quantum Matter (CICQM), Beijing, China.

^oAlso at Department of Physics, Ben Gurion University of the Negev, Beer Sheva, Israel.

- ^pAlso at Università di Napoli Parthenope, Napoli, Italy.
- ^qAlso at Institute of Particle Physics (IPP), Canada.
- ^rAlso at Borough of Manhattan Community College, City University of New York, New York, New York, USA.
- ^sAlso at National Institute of Physics, University of the Philippines Diliman (Philippines), Philippines.
- ^tAlso at Department of Financial and Management Engineering, University of the Aegean, Chios, Greece.
- ^uAlso at Department of Physics, Stanford University, Stanford, California, USA.
- ^vAlso at Centro Studi e Ricerche Enrico Fermi, Italy.
- ^wAlso at Institutio Catalana de Recerca i Estudis Avancats, ICREA, Barcelona, Spain.
- ^xAlso at Technical University of Munich, Munich, Germany.
- ^yAlso at Department of Physics and Astronomy, University of Sheffield, Sheffield, United Kingdom.
- ^zAlso at Yeditepe University, Physics Department, Istanbul, Türkiye.
- ^{aa}Also at Institute of Theoretical Physics, Ilia State University, Tbilisi, Georgia.
- ^{bb}Also at CERN, Geneva, Switzerland.
- ^{cc}Also at Center for Interdisciplinary Research and Innovation (CIRI-AUTH), Thessaloniki, Greece.
- ^{dd}Also at Hellenic Open University, Patras, Greece.
- ^{ee}Also at Center for High Energy Physics, Peking University, China.
- ^{ff}Also at APC, Université Paris Cité, CNRS/IN2P3, Paris, France.
- ^{gg}Also at IRFU, CEA, Université Paris-Saclay, Gif-sur-Yvette, France.
- ^{hh}Also at Department of Physics, Royal Holloway University of London, Egham, United Kingdom.
- ⁱⁱAlso at L2IT, Université de Toulouse, CNRS/IN2P3, UPS, Toulouse, France.
- ^{jj}Also at Department of Physics, California State University, Sacramento, California, USA.
- ^{kk}Also at Département de Physique Nucléaire et Corpusculaire, Université de Genève, Genève, Switzerland.
- ^{ll}Also at Deutsches Elektronen-Synchrotron DESY, Hamburg and Zeuthen, Germany.
- ^{mm}Also at Fakultät für Mathematik und Naturwissenschaften, Fachgruppe Physik, Bergische Universität Wuppertal, Wuppertal, Germany.
- ⁿⁿAlso at Institute for Nuclear Research and Nuclear Energy (INRNE) of the Bulgarian Academy of Sciences, Sofia, Bulgaria.
- ^{oo}Also at Washington College, Chestertown, Maryland, USA.
- ^{pp}Also at School of Physics and Astronomy, University of Birmingham, Birmingham, United Kingdom.
- ^{qq}Also at Institut für Experimentalphysik, Universität Hamburg, Hamburg, Germany.
- ^{rr}Also at Institute of Applied Physics, Mohammed VI Polytechnic University, Ben Guerir, Morocco.
- ^{ss}Also at Institute of Physics and Technology, Ulaanbaatar, Mongolia.
- ^{tt}Also at Department of Physics and Astronomy, Michigan State University, East Lansing, Michigan, USA.